Journal of Ambient Intelligence and Humanized Computing (2023) 14:7109–7131
https://doi.org/10.1007/s12652-021-03564-4

ORIGINAL RESEARCH

Opposition decided gradient-based optimizer with balance analysis and diversity maintenance for parameter identification of solar photovoltaic models

M. Premkumar[1] · Pradeep Jangir[2] · Rajvikram Madurai Elavarasan[3] · R. Sowmya[4]

Received: 15 March 2021 / Accepted: 17 October 2021 / Published online: 1 November 2021

Abstract

The solar photovoltaic (PV) parameter estimation/identification is a complicated optimization process that directly affects the performance of PV systems if the internal parameters of PV cells are not estimated accurately. Finding the precise and accurate parameters of PV models is the primary gateway to the PV system design to mimic their actual behavior. Numerous optimization algorithms are used to find the cell/module parameters, however, most of these algorithms suffer from the high computational burden, local optima trap, and frequent parameter tuning to get the best results. A metaheuristic algorithm called gradient-based optimization algorithm (GOA) is recently introduced to solve numerical optimization and engineering design problems. Nevertheless, the GOA appears to be trapped in sub-optimal locations, increasing computational time to get the best results. Thus, this paper recommends an enhanced GOA by employing an opposition-based learning mechanism to generate more precise solutions. Therefore, this paper proposes an enhanced variant, called opposition-based GOA (OBGOA), to identify the electrical parameters of various PV models, such as the single-diode model (SDM) and double-diode model (DDM). Numerous experimental data profiles are considered to classify the parameters of the SDM and DDM. The obtained results show that the OBGOA can estimate accurate and precise parameters than the other algorithms. In addition, statistical data analysis of various algorithms is presented for all the PV models. The results demonstrated that the proposed OBGOA could find circuit parameters of the cell and the modules accurately and effectively. This study is backed up by additional online guidance and support at https://premkumarmanoharan.wixsite.com/mysite.

Keywords Gradient-based optimization algorithm (GOA) · Opposition-based learning · Opposition-based gradient-based optimization algorithm (OBGOA) · Parameter estimation · PV models

List of symbols

I_p	Photocurrent in A
I_d	Diode current in A
I_{sh}	Current through the shunt resistor in A
I	Output current of the cell/module in A
V	Output voltage of the cell/module in V
I_{sd}, I_{sd1}, and I_{sd2}	Reverse saturation current of the diodes in A
R_p and R_s	Ohmic resistance of the cell in Ω
n, n_1, and n_2	Ideality factor of diodes
D	Problem dimension
$X1_n^t$	Updated position of the population
x_{best} and x_{worst}	Best and worst solutions, respectively
r_1,r_2,r_3, and r_4	Random integers between [0, D]
P_r	Probability rate
q	Electron charge in C
k	Boltzmann constant in J/K
T	Absolute temperature in K
N_s and N_{sh}	Series- and parallel-connected cells, respectively
X	Number of data samples
Y	Number of decision variables

✉ M. Premkumar
mprem.me@gmail.com

[1] Department of Electrical and Electronics Engineering, Dayananda Sagar College of Engineering, Bengaluru, Karnataka 560078, India

[2] Rajasthan Rajya Vidyut Prasaran Nigam Ltd., Sikar, Rajasthan 332025, India

[3] Department of Electrical and Electronics Engineering, Thiagarajar College of Engineering, Madurai, Tamil Nadu 625015, India

[4] Department of Electrical and Electronics Engineering, National Institute of Technology, Tiruchirappalli, Tamil Nadu 620015, India

N_p	Population size
IT_{max}	Maximum number of iterations
X_{ub} and X_{lb}	Upper and lower boundary limit
x_p^t	Randomly selected solution
$\overline{X}$	Random opposite solution
I_{exp}	Experimental current sample in A
I_{est}	Estimated current in A

Abbreviations

PV	Photovoltaic
GOA	Gradient-based optimization algorithm
OBL	Opposition-based learning
OBGOA	Opposition-based GOA
SDM	Single-diode model
DDM	Double-diode model
RES	Renewable energy systems
STC	Standard test condition
TDM	Three-diode model
IJAYA	Improved Jaya algorithm
TLBO	Teaching–learning-based optimization
PSO	Particle swarm optimization
FPA	Flower pollination algorithm
ALO	Ant lion optimization
MFO	Moth-flame optimization
BFA	Bacterial foraging algorithm
SFLA	Shuffled frog leaping algorithm
FFO	Firefly optimization
GWO	Grey wolf optimization
WOA	Whale optimization algorithm
SCA	Sine–cosine algorithm
SSA	Salp-swarm algorithm
COA	Coyote optimization algorithm
HHO	Harris Hawks optimizer
SMA	Slime mould algorithm
EO	Equilibrium optimizer
DE	Differential evolution
ABC	Artificial Bee Colony
MPA	Marine-predator algorithm
RMSE	Root mean square error
GSR	Gradient search rule
DM	Direction of movement
LEO	Local escaping operator
NFL	No-free-lunch
RE	Relative error
IAE	Integral absolute error

1 Introduction

Renewable energy systems (RES) are growing global interest as fossil fuel resources are depleted, electricity demand is increasing in developing countries, and costs of the photovoltaic (PV) modules have been reduced. Solar energy is the most popular source of energy that includes several applications such as irrigation, solar farming, street light, water heating, and is another most popular RES. The significant advantage of the PV system is that it can convert solar energy directly to a direct current. PV systems, including standalone, grid-tied, and hybrid systems, have a broad range of options (Premkumar et al. 2020c, d). Using an exact model with respect to the experimental I–V data, the most significant task is to improve the PV system performance throughout the operation. The cell manufacturers verify the I–V curve against standard test conditions (STC). The performance of the PV system can be severely impacted by ambient pressure, temperature, and irradiance changes in the environment (Premkumar et al. 2020b). Therefore, several PV models are proposed, such as the single-diode model (SDM), double-diode model (DDM), and three-diode model (TDM), to analyze the behavior of the PV cell/module. Such models differ in precision or complexity, with the most frequently accepted models being the SDM and DDM. In general, the precision of the PV system is dependent upon the model parameters, so it is necessary to estimate such parameters in order to maximize the effectiveness (Chin et al. 2015).

Using different optimization methods that can be classified as analytical, deterministic, and metaheuristic methods, investigators have attempted to improve the operation of the PV system. In order to define the value of unknown variables, the analytical methods use several mathematical formulas (Navabi et al. 2015; Batzelis and Papathanassiou 2016). Although the ease of processing and rate of getting the results, the analytical techniques could be unreliable and, depending on certain assumptions planned in advance within STC (Wolf and Benda 2013), lead to a significant gap between the measured and simulated output of the real PV model. The methods, such as the Newton–Raphson, Lambert W-functions, etc., are few examples of deterministic approaches that include limitations on the design, including convexity and differentiability. Identifying the PV model parameters is multi-modal and non-linear, which causes the deterministic approaches to fall towards premature convergence and can lead to low output if the initial parameters are far from the global solutions (Ishaque et al. 2012; Liang et al. 2020).

To overcome the deficiency in existing techniques, metaheuristic techniques are considered to obtain the most promising solution to the PV parameter identification optimization problem. Consequently, to prevent stagnation in the local minimum, they must balance both the exploitation and exploration phases (Li et al. 2020). The various real-world applications were motivated by the exceptional advancement of metaheuristic techniques and the significance of solar power and its variety of real-world applications to devise a new metaheuristic optimization to identify the PV model parameters (Wong and Ming 2019). Different optimization techniques have been successfully used to characterize the photovoltaic system with such PV parameters, including differential evolution (DE) algorithm (Xiong et al. 2018b), genetic algorithm (GA) (Kumari and Geethanjali 2017), Jaya algorithm (Venkata Rao 2016), improved Jaya algorithm (IJAYA) (Yu et al. 2017b; Premkumar et al. 2021b), Rao algorithm (Premkumar et al. 2020a), teaching–learning-based optimization (TLBO) algorithm (Liao et al. 2020), particle swarm optimization (PSO) algorithm (Khanna et al. 2015), gravitational search algorithm (Mosavi et al. 2019), stochastic fractal search algorithm (Khishe et al. 2018), autonomous PSO (Mosavi and Khishe 2017), Artificial Bee Colony (ABC) (Jamadi et al. 2016), biogeography-based optimization (Kaveh et al. 2019; Mosavi et al. 2017), moth-flame optimization (MFO) algorithm (Sheng et al. 2019), bacterial foraging algorithm (BFA) (Krishnakumar et al. 2013), shuffled frog leaping algorithm (SFLA) (Hasanien 2015), cuckoo search (CS) (Yang and Deb 2010), firefly optimization (FFO) (Louzazni et al. 2017), grey wolf optimization (GWO) algorithm (Long et al. 2020), whale optimization algorithm (WOA) (Oliva et al. 2017; Khishe and Mosavi 2019; Qiao et al. 2021), sine–cosine algorithm (SCA) (Montoya et al. 2020), salp-swarm algorithm (SSA) (Abbassi et al. 2019; Khishe and Mohammadi 2019), coyote optimization algorithm (COA) (Diab et al. 2020), dragonfly optimization (Khishe and Safari 2019), Harris Hawks optimizer (HHO) (Jiao et al. 2020), marine-predator algorithm (MPA) (Soliman and Hasanien 2020), slime mould algorithm (SMA) (Kumar et al. 2020), equilibrium optimizer (Abdel-basset et al. 2020), and chimps optimization (Khishe and Mosavi 2020a, b). A detailed review of all the algorithms for the solar parameter estimation problem is provided as a supplementary file.

Ishaque and Salam (2011) introduced the DE to calculate the model parameters at various irradiances and temperatures for several types of photovoltaic cells. Ishaque et al. (2012) introduced a penalty-based DE algorithm to determine the variables of the module using artificial data. The authors of Biswas et al. (2019) suggested that the L-SHADE method adjusts its variables based on the performance history of such variables in past iterations. Yu et al. (2017a) presented a self-adaptive TLBO technique that accurately assesses the PV model parameters. The findings found that compared to other comparative approaches, the suggested technique demonstrates sharpness and high precision. Besides, the BFA (Rajasekar et al. 2013) has been implemented with new objective functions to determine maximum power and open-circuit voltage that help to estimate characteristics of the solar PV cell/module correctly. The SCA technique is integrated with the Nelder-Mead simplex method and the learning system based on the opposition to improve the solution accuracy (Chen et al. 2019). Xiong et al. (2018a) suggested a different extraction approach based on using enhanced WOA to obtain the parameters of different PV models selectively. The traditional WOA has good local search exposure, but it struggles from premature convergence when dealing with numerous multi-modal issues. Allam et al. (2016) introduced an optimized method of parameter optimization using the MFO algorithm. The suggested technique has been applied to estimate the three models (i.e., SDM, DDM, and TDM) based on data measured in the research laboratory.

Metaheuristics are not optimal, with a few of these having many problems affecting the accuracy and efficiency. The opposition-based learning (OBL) mechanism was already implemented to prevent these conditions and the OBL considers the solution of the individual candidate and produces the opposite position in the search space (Tizhoosh 2005). The OBL validates whether the candidate solution or the opposite function has the best value of the objective function through a single rule. This method might be implemented at initialization or when the population changes a pair of possible results based on the procedure. The OBL has shown that effectiveness enhances many metaheuristic algorithms. For numerical solution space, the firefly algorithm has also been updated using OBL (Verma et al. 2016). The opposition-based rule was also used to determine the parameters using the SFLA in industrial automation (Ahandani and Alavi-Rad 2015). Many of these experiments demonstrate that OBL is an exciting process for optimization problems to produce better performance.

The gradient-based optimization algorithm (GOA) is a recently reported metaheuristic algorithm (Ahmadianfar et al. 2020). And it has been developed for a numerical optimization problem. However, when GOA is applied to real-world engineering problems, including solar parameter estimation problems, the GOA suffers due to the local optima trap. To avoid this trapping and to improve the convergence rate of the basic GOA, the OBL scheme is integrated with the GOA to formulate a new algorithm called opposition-based gradient-based optimization algorithm (OBGOA). The no-free lunch (NFL) theory states that no optimization algorithm can outperform another on any measure across all problems (Wolpert and Macready 1997). However, OBGOA can quickly distinguish between the exploration and exploitation phases and converges on more accurate results. This study proposes the use of OBGOA to extract the electrical parameters of the PV cell and module with high accuracy and in real-time, based on the arguments stated in the NFL theory OBGOA's capacity to regulate the exploitation and exploration phases. The key contributions of this paper are as follows.

- The usage of OBL, in conjunction with GOA, greatly increases the accuracy and efficiency of the traditional GOA. However, such enhancement meets the limitations of the GOA, retaining the excellent potential for optimization.

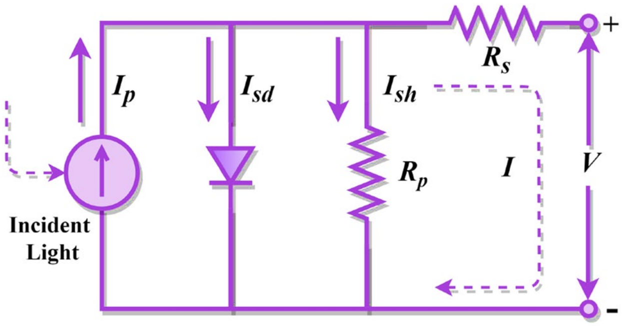

Fig. 1 Single-diode photovoltaic cell model

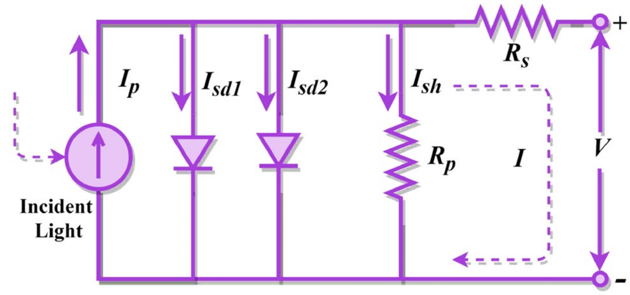

Fig. 2 Double-diode photovoltaic cell model

- To prove that the proposed OBGOA can solve real-time applications, the proposed algorithm is validated over the solar PV parameter estimation problem.
- Comparisons with several other existing techniques revealed that in terms of effectiveness and accuracy, the OBGOA could produce positive performance.
- Various metrics and statistical validations support the experiments and comparisons.

The rest of the paper is structured as follows. Section 2 presents a mathematical model of the single-diode and double-diode model of the photovoltaic cell/module, in addition to the objective function formulation for the above-said problem. Section 3 briefly explains the basic concepts of the traditional GOA and describes the development process of the proposed OBGOA. Section 4 discusses the experimental results and the performance comparison with other metaheuristic techniques. Finally, the findings are provided in Sect. 5 with concluding remarks.

2 Mathematical model of the photovoltaic cell/module and problem formulation

Several PV models have defined the I–V characteristics of the solar cell and panel. SDM and DDM are the most widely used models in practical applications. This section presents the photovoltaic cell and module's equivalent circuit for both SDM and DDM, along with the objective functions (Mohamed et al. 2013; Drouiche et al. 2018).

2.1 Single-diode model (SDM) of the PV cell

The single-diode model has been widely utilized in numerous applications, particularly when defining the characteristics of the PV cell. The equivalent circuit of the single diode model is illustrated in Fig. 1, including photocurrent I_p, the current through the diode I_d, and shunt resistor current I_{sh}. Furthermore, in Eq. (1), the output current (I) is described.

$$I = I_p - I_d - I_{sh} \tag{1}$$

As per the Shockley equation, the diode current I_d is given in Eq. (2), in which the reverse saturation current of the diode is denoted as I_{sd}, the ohmic resistance of the PV cell is represented as R_p and R_s, the output voltage of the PV cell is V, the output current is I, and the diode ideality factor is denoted n. In addition, the expression for I_{sh} is presented in Eq. (3).

$$I_d = I_{sd}\left[\exp\left(\frac{q(V + IR_s)}{nkT}\right) - 1\right] \tag{2}$$

$$I_{sh} = \frac{V + IR_s}{R_p} \tag{3}$$

where the electron charge q is equal to $1.602*10^{-19}$ C, the Boltzmann constant k equals $1.3806*10^{-23}$ J/K, and the absolute temperature is denoted as T in Kelvin. Therefore, Eq. (1) is rewritten as follows.

$$I = I_p - I_{sd}\left[\exp\left(\frac{q(V + IR_s)}{nkT}\right) - 1\right] - \frac{V + IR_s}{R_p} \tag{4}$$

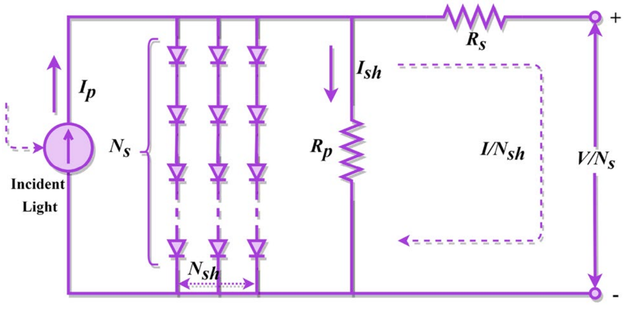

Fig. 3 Equivalent circuit of the solar PV module

The five unknown parameters of the SDM of the PV cell is observed from Eq. (4) and is presented as I_p, I_{sd}, n, R_s and R_p.

2.2 Double-diode model (DDM) of the PV cell

The DDM is established considering the impact of the recombination losses in the depletion region. In the double-diode model, the controlled current source has two diodes connected in parallel and parallel resistance. The circuit structure of the DDM is shown in Fig. 2. The total photovoltaic cell current is given as follows.

$$I = I_p - I_d - I_{sh} = I_p - I_{sd1}\left[\exp\left(\frac{q\left(V + IR_s\right)}{n_1 kT}\right) - 1\right] - I_{sd2}\left[\exp\left(\frac{q\left(V + IR_s\right)}{n_2 kT}\right) - 1\right] - \frac{V + IR_s}{R_p} \tag{5}$$

The reverse saturation current and the diffusion current are denoted as I_{sd1} and I_{sd2}, and the diffusion and recombination diode ideality factors are denoted as n_1 and n_2. The seven unknown parameters of the DDM of the PV cell is observed from Eq. (5) and is presented as $I_p, n_1, n_2, I_{sd1}, I_{sd2}, R_s$, and R_p.

2.3 Mathematical models of the solar photovoltaic module

The PV module contains multiple series or parallel cells whose arrangement is shown in Fig. 3. The PV module focused on SDM and DDM can be defined by Eqs. (6) as well as (7).

The series-connected PV cells are referred to as N_s, the parallel-connected PV cells are referred to as N_{sh}, the total voltage of the module is referred to as V, and the total current of the module is referred to as I.

2.4 Objective function formulation

To optimize the model parameters from the estimated current and the variation between experimental current, identifying the PV cell parameters for various models is probably converted into an optimization problem. During the optimization procedure, the current of the PV cell/module is obtained by optimizing the design variables. First, identify the optimal values of unknown parameters, as previously discussed, such that the error between the estimated current and the experimental current is as minimal as possible. Equation (8) introduces the fitness function of the optimization problem, which would also be considered the root mean square error (RMSE) (Jordehi 2016). Owing to its non-linear transcendental nature, the fitness function is challenging to solve. This study's key objective is to check for a vector Y that allows the *RMSE(Y)* value to achieve the lowest value.

$$RMSE\left(Y_i\right) = \sqrt{\frac{1}{X}\sum_{k=1}^{X} f_k\left(V, I, Y_i\right)^2} \tag{8}$$

The number of samples is referred to as X, and the decision/optimization/design variables are referred to as Y.

3 Improved gradient-based optimization algorithm

This section of the paper briefly introduces the concept of the GOA and extend the discussions to the formulation of the OBGOA.

$$I = I_p N_{sh} - I_{sd} N_{sh}\left[\exp\left(\frac{q(V + IR_s\left(N_s/N_{sh}\right))}{N_s nkT}\right) - 1\right] - \frac{V + IR_s\left(N_s/N_{sh}\right)}{R_p\left(N_s/N_{sh}\right)} \tag{6}$$

$$I = I_p N_{sh} - I_{sd1} N_{sh}\left[\exp\left(\frac{q(V + IR_s\left(N_s/N_{sh}\right))}{N_s n_1 kT}\right) - 1\right] - I_{sd2} N_{sh}\left[\exp\left(\frac{q(V + IR_s\left(N_s/N_{sh}\right))}{N_s n_2 kT}\right) - 1\right] - \frac{V + IR_s\left(N_s/N_{sh}\right)}{R_p\left(N_s/N_{sh}\right)} \tag{7}$$

3.1 Gradient-based optimization algorithm (GOA)

In the traditional GOA that incorporates the gradient and population-based methods, Newton's approach for exploring the search domain using a set of variables and two major operators, such as local escaping operators and gradient search rule, define the search path (Ahmadianfar et al. 2020). The initialization phase of the GOA is similar to other metaheuristics algorithms. Therefore, the initialization phase is not discussed in this paper.

3.1.1 Gradient search rule (GSR)

The migration of vectors is supervised in the gradient search rule (GSR) to improve search in the possible area and obtain good positions. The GSR allows the GOA to adjust for the random actions during the optimization procedure, supporting exploration and avoiding premature convergence. The convergence rate of the GOA technique is facilitated using the direction of movement (DM) to establish an acceptable local search propensity. Therefore, the current vector position is updated using Eq. (11).

$$X1_n^t = x_n^t - GSR + DM \tag{9}$$

$$GSR = randn \times \rho_1 \times \frac{2\Delta x \times x_n^t}{\left(x_{\mathrm{worst}} - x_{best} + \varepsilon\right)} \tag{10}$$

$$DM = rand \times \rho_2 \times \left(x_{best} - x_n^t\right) \tag{11}$$

The current vector x_n^t is updated using Eq. (9), and the newly updated vector is denoted as $X1_n^t$. The term ρ_1 is the critical control parameter to balance the exploitation and exploration phases. The best solution and the worst solutions during the optimization are represented as x_{best} and x_{worst}, respectively. The value of ε is inside the range of [0, 0.1]

$$\rho_1 = 2 \times rand \times \alpha - \alpha \tag{12}$$

$$\alpha = \left|\beta \times \sin\left(\frac{3\pi}{2} + \sin\left(\beta \times \frac{3\pi}{2}\right)\right)\right| \tag{13}$$

$$\beta = \beta_{\min} + \left(\beta_{\max} - \beta_{\min}\right) \times \left(1 - \left(\frac{t}{IT_{\max}}\right)^3\right)^2 \tag{14}$$

where the current iteration is denoted as t, the values of $\beta_{\max}$ and $\beta_{\min}$ are equal to 1.2 and 0.2, respectively, and *randn* is a uniformly distributed random number. The difference between the randomly selected position and the current best solution is represented as Δx. The variable δ has been presented to verify that the Δx is changed during each iteration.

$$\delta = 2 \times rand \times \left|\frac{x_{r_1}^t + x_{r_2}^t + x_{r_3}^t + x_{r_4}^t}{4} - x_n^t\right| \tag{15}$$

where *rand* is a random number with D-dimensions, the integers, such as r_1,r_2,r_3, and $r_4 (r_1 \neq r_2 \neq r_3 \neq r_4 \neq n)$ are randomly selected between [1, D]. Another random parameter that supports the exploration phase of the GOA is referred to as ρ_2 and it helps each vector in the population to have various step sizes. The expression for ρ_2 as follows.

$$\rho_2 = 2 \times rand \times \alpha - \alpha \tag{16}$$

After introducing Newton's method to improve the exploration and diversity and generate a strong population-based search process, Eq. (9) can be rewritten as follows.

$$X1_n^t = x_n^t - randn \times \rho_1 \times \frac{2\Delta x \times x_n^t}{\left(yp_n^t - yq_n^t + \varepsilon\right)} + rand \times \rho_2 \times \left(x_{best} - x_n^t\right) \tag{17}$$

Replace the best vector position with the current vector position in Eq. (17). Therefore, a new vector ($X2_n^t$) is generated, and it is expressed as follows.

$$X2_n^t = x_{\mathrm{best}} - randn \times \rho_1 \times \frac{2\Delta x \times x_n^t}{\left(yp_n^t - yq_n^t + \varepsilon\right)} + rand \times \rho_2 \times \left(x_{r1}^t - x_{r2}^t\right) \tag{18}$$

$$yp_n = rand \times \left(\frac{\left[z_{n+1} + x_n\right]}{2} + rand \times \Delta x\right) \tag{19}$$

$$yq_n = rand \times \left(\frac{\left[z_{n+1} + x_n\right]}{2} - rand \times \Delta x\right) \tag{20}$$

The search process as represented in Eq. (18) is useful for local search but is restricted to global search, while Eq. (17) implemented the search process that is perfect for global search, but local search is restricted. Therefore, to improve both the exploration and exploitation ability of the algorithm, both search strategies are utilized in GOA. Based on Eqs. (17) and (18), along with the current vector position, the updated solution during the next iteration x_n^{t+1} is written as follows.

$$x_n^{t+1} = r_a \times \left(r_b \times X1_n^t + \left(1 - r_b\right) \times X2_n^t\right) + \left(1 - r_a\right) \times X3_n^t \tag{21}$$

$$X3_n^t = X_n^t - \rho_1 \times \left(X2_n^t - X1_n^t\right) \tag{22}$$

3.1.2 Local escaping operator (LEO)

The LEO is applied to facilitate the validity of the GOA in solving difficult problems. By exploiting numerous probable solutions, the LEO produces a superior solution X_{LEO}^t including random solutions, such as x_{r1}^t and x_{r2}^t, the position of the best solution x_{best}, updated random solution x_k^t, and the solutions $X1_n^t$ and $X2_n^t$.

$$\begin{array}{l}
\textbf{if } \ rand < P_r \\
\quad \textbf{if } rand < 0.5 \\
\qquad X_{LEO}^t = X_n^{t+1} + a \times \left(u_1 \times x_{\text{best}} - u_2 \times x_k^t\right) + b \times \rho_1 \times \left(u_3 \times \left(X2_n^t - X1_n^t\right) + u_2 \times \left(x_{r1}^t - x_{r2}^t\right)\right)/2 \\
\qquad X_n^{t+1} = X_{LEO}^t \\
\quad \textbf{else} \\
\qquad X_{LEO}^t = x_{\text{best}} + a \times \left(u_1 \times x_{\text{best}} - u_2 \times x_k^t\right) + b \times \rho_1 \times \left(u_3 \times \left(X2_n^t - X1_n^t\right) + u_2 \times \left(x_{r1}^t - x_{r2}^t\right)\right)/2 \\
\qquad X_n^{t+1} = X_{LEO}^t \\
\quad \textbf{end} \\
\textbf{end}
\end{array} \tag{23}$$

The value of a is a uniform random number in the range of $[-1, 1]$, the value of b is a normal distributed random number with a standard deviation (SD) of 1 and a mean of 0, P_r is the probability rate, and the random numbers, such as u_1, u_2, and u_3 are written as follows.

$$u_1 = \begin{cases} 2 \times rand, \, if\, \mu_1 < 0.5 \\ 1, otherwise \end{cases} \tag{24}$$

$$u_2 = \begin{cases} rand, \, if\, \mu_1 < 0.5 \\ 1, otherwise \end{cases} \tag{25}$$

$$u_3 = \begin{cases} rand, \, if\, \mu_1 < 0.5 \\ 1, otherwise \end{cases} \tag{26}$$

The value of μ_1 is varies between [0, 1] and *rand* is a random number between [0, 1]. Equations (24–26) are rewritten as follows.

$$u_1 = L_1 \times 2 \times rand + \left(1 - L_1\right) \tag{27}$$

$$u_2 = L_1 \times rand + \left(1 - L_1\right) \tag{28}$$

$$u_3 = L_1 \times rand + \left(1 - L_1\right) \tag{29}$$

The value of L_1 is 0 when the value of μ_1 is larger than or equal to 0.5; otherwise, the value is 1. The following update scheme is used in Eq. (23) to find the solution x_k^t.

$$x_k^t = \begin{cases} x_{rand}, \, if\, \mu_2 < 0.5 \\ x_p^t, otherwise \end{cases} \tag{30}$$

$$x_{rand} = X_{lb} + rand \times (X_{ub} - X_{lb}) \tag{31}$$

where μ_2 is a random number between [0, 1], the randomly selected population solution is x_{rand}, and the new solution is x_p^t. Therefore, Eq. (30) is rewritten as follows.

$$x_k^t = L_2 \times x_p^t + \left(1 - L_2\right) \times x_{rand} \tag{32}$$

As similar to L_1, L_2 is also a binary parameter. The value of L_2 is 0 when the value of μ_2 is larger than or equal to 0.5; otherwise, the value is 1. The pseudocode of the basic version of the GOA is shown in the *Algorithm*.

Algorithm: Pseudocode of the GOA

```
Step 1: Initialization Stage
        Assign values for parameters Pr, ε, and ITmax
        Evaluate the objective function value, f(Xn), n=1, 2, …, Np
        Specify the worst and best solutions, x^t_worst and x^t_best
Step 2: Main Loop
        While (t< ITmax)
            for n = 1:Np
                Select randomly r1 ≠ r2 ≠ r3 ≠ r4 ≠ n in the range of [1, Np]
                Find the position x^{t+1}_{i,n} using Eq. 29
            end for
            if rand < Pr    [Local Escaping Operator (LEO)]
                Find the position x^t_LEO using Eq. 31
                X^{t+1}_n = x^t_LEO
            end if
                Update the worst and best solutions, x^t_worst and x^t_best
            end for
        end while
Return the best solution
```

3.2 Opposition-based learning (OBL)

The opposition-based learning concept has been adopted to enhance the integration of heuristic approaches to explore a global optimization solution. Generally, the metaheuristic approaches generate the initial population and random

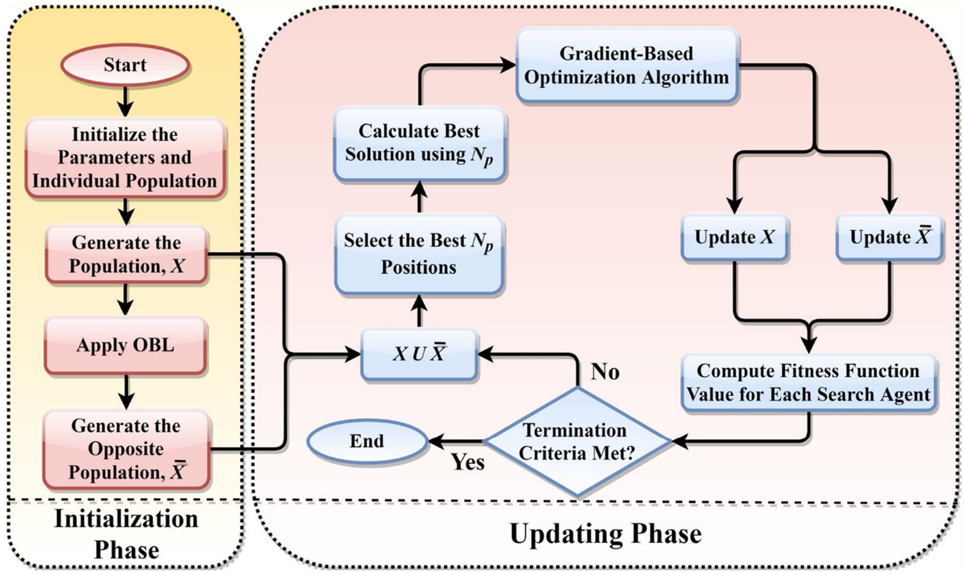

Fig. 4 Flowchart of the proposed OBGOA

solutions to discover the optimal solution. However, the initial solutions are randomly generated or based on previous information, including specifying domain search or other parameters. In the lack of such information, these methods can neither converge to a global optimal because their function is randomly in the solution space. Such methods are often laborious since they rely on the difference between current and best solutions. The OBL proposes a technique to try for a solution oppositely to the current solution to overcome these problems, so the solution gets nearer to the desired solution, and the convergence gets smoother (Cuevas et al. 2012). The opposite value of the real number $x \in [lb, ub]$ is denoted as $\bar{x}$ and is given in Eq. (33).

$$\bar{x} = ub + lb - x \tag{33}$$

For the multi-dimensional search space, Eq. (33) is rewritten as follows.

$$\overline{x_i} = ub_i + lb_i - x_i, i = 1, 2, \ldots, D \tag{34}$$

The opposite point $\overline{x_i}$ is replaced with the respective solution x depending on the fitness function value. If $f(x)$ is greater than $f(\bar{x})$, then x does not alter, else $x = \bar{x}$; thus, population solutions are changed based on the better value of $\bar{x}$ and x.

3.3 Proposed opposition-based gradient-based optimization algorithm (OBGOA)

A few limitations of the conventional GOA are being trapped in the optimal local solution, high computational complexity, and poor convergence and such restrictions are attributable to the fact that specific solutions are modified to the optimal solution though few solutions are removed from this solution. However, when taking the opposite solution into account, the OBGOA removes these disadvantages. Besides, the OBGOA integrates the basic GOA's search functionality with the OBL to improve solution space exploration. Thus, the proposed technique has fewer parameters to be adjusted relative to similar techniques, and the introduction of OBL doesn't impact the GOA specification, while on the other hand, the reliability of the optimum solution is improved. In this context, the size of the initial population owing to enhancing convergence can be reduced to the best solution, as OBGOA can discover the search space widely.

Nevertheless, the OBGOA population setting may also influence the call functions provided in the optimization problem. An assessment of the objective function requires more computation time, relying on the execution. This reality explicitly correlates to the NFL statement, stating that an algorithm cannot be enhanced without losing any benefit. This is the primary reason to create OBGOA. The suggested methodology enhances the GOA over two phases: primarily, the OBL has been utilized to increase the rate of converge in the population initialization and stop trapped in local optimal by looking for solutions in the entire search space. Second, the OBL has been used in updating the population approach to test whether the change in the opposite track is higher than the current improvement. The suggested strategy randomly generates the population X with size N_p, in which the solution $x_j = [x_{j1}, x_{j2}, \ldots, x_{jD}]$, $j = 1, 2, \ldots, N_p$. Therefore, each opposite solution is determined by OBL, and afterward, the opposite population $\bar{X}$ is developed. The optimal N_p solution is chosen based on the $\bar{X}$ and X populations.

Phase I: initialization phase

Table 1 Upper and lower bounds for PV models

Parameters	RTC Si solar cell		PhotoWatt-PWP201		SM55, KC200GT	
	ub	*lb*	*ub*	*lb*	*ub*	*lb*
I_p (A)	1	0	2	0	$2I_{sc}$	0
I_{sd}, I_{sd1}, I_{sd2} (A)	1e – 06	0	50e – 06	0	100e – 06	0
n, n_1, n_2	1	2	1	50	1	5
R_p (Ω)	100	0	2000	0	5000	0
R_s (Ω)	0.5	0	2	0	2	0

Table 2 Uncertain parameters estimated by various algorithms for SDM of the cell (RTC France Si solar cell)

Algorithm	I_p (A)	I_{sd} (μA)	R_s (Ω)	R_p (Ω)	n	*RMSE*	*sig*
SSA	0.7658	9.98E – 07	0.0301	29.06	1.6059	2.093E – 03	+
COA	0.7605	3.56E – 07	0.0362	63.40	1.4909	1.1022E – 03	+
SMA	0.7602	1.97E – 07	0.0384	54.31	1.4326	1.3823E – 03	+
EO	0.7610	4.31E – 07	0.0351	57.84	1.5108	1.0510E – 03	+
HHO	0.7609	1.46E – 07	0.0394	40.75	1.4053	8.7964E – 03	+
MPA	0.7612	4.12E – 07	0.0353	52.84	1.5062	1.5219E – 03	+
GOA	0.7606	3.79E – 07	0.0358	60.78	1.4975	9.9239E – 04	+
Proposed	**0.7608**	**3.23E – 07**	**0.0364**	**53.72**	**1.4812**	**9.8602E – 04**	

i. Initialize the random population solutions X.
ii. Determine the opposite population $\overline{X}$ as follows.

$$\overline{x_{n,i}} = ub_{n,i} + lb_{n,i} - x_{n,i}, i = 1, 2, \dots, D, n = 1, 2, \dots, N_p$$

iii. Choose the best population solutions from $X \cup \overline{X}$ to generate a new population.

Phase II: updated phase—After deciding the proper population solutions that have created a new population, the OBGOA decides the optimal population solution. Using the GOA, the population solution X is revised, and the objective functions are measured, and the opposite population $\overline{X}$ is calculated based on the OBL, and the objective function is assessed for each $\overline{x}$. Focused on the objective function, the next stage in the OBGOA is to choose the best population solutions from $X \cup \overline{X}$. The processes are repeated till the stopping conditions, as shown in Fig. 4.

4 Experimental results and discussions

This section shows the effectiveness of the proposed OBGOA, and the experimental findings were presented. The OBGOA is mainly implemented in three different models: SDM, DDM, and PV models, to estimate uncertain parameters. The description of the datasets used is discussed as follows. The experimental data samples of RTC France Si solar cell, PhotoWatt-PWP201, KC200GT, and SM55 are considered to examine the effectiveness of the proposed algorithm. The first set from which includes 26 samples of voltage and current are obtained from an RTC France Si solar cell at an irradiance of 1000 W/m^2 and temperature of 33 °C (Premkumar et al. 2021a), and the second set is the data obtained from a PhotoWatt-PWP201 module (Premkumar et al. 2021a). Two commercial versions are also being evaluated: monocrystalline SM55 (Chaibi et al. 2019) and

Table 3 Uncertain parameters estimated by various algorithms for DDM of the cell (RTC France Si solar cell)

Algorithm	I_p (A)	I_{sd1} (μA)	R_s (Ω)	R_p (Ω)	n_1	I_{sd2} (μA)	n_2	*RSME*	*sig*
SSA	0.7610	2.6520E – 07	0.0367	50.695	1.46393	3.09E – 07	1.980584	3.1102E – 04	+
COA	0.7601	2.6714E – 07	0.0365	70.556	1.467289	2.57E – 07	1.818639	2.3421E – 03	+
SMA	0.7598	2.0263E – 08	0.0345	99.802	1.955814	5.30E – 07	1.532801	3.1367E – 03	+
EO	0.7598	3.0068E – 07	0.0360	81.602	1.478448	5.23E – 07	1.952979	3.0240E – 03	+
HHO	0.7593	1.4142E – 07	0.0361	99.618	1.523704	2.65E – 07	1.495437	3.7640E – 03	+
MPA	0.7608	3.7511E – 08	0.0344	70.873	1.773231	5.13E – 07	1.530335	2.1920E – 03	+
GOA	0.7608	1.2550E – 07	0.0364	53.762	1.51139	2.02E – 07	1.468685	9.8602E – 04	+
Proposed	**0.7608**	**2.2021E – 07**	**0.0368**	**55.8326**	**1.4489**	**8.02E – 07**	**2.0000**	**9.8258E – 04**	

multi-crystalline KC200GT (Ma 2014), from the manufacturer's datasheet to show the robustness and accuracy of the OBGOA at various temperature and irradiance levels. The findings of which would be contrasted to those of other successful and very recent algorithms, such as EO, GOA, MPA, SMA, COA, SSA, and HHO. The OBGOA and other algorithms are executed using MATLAB software installed on a laptop with a 2.44 GHz clock frequency and 8 GB of memory. Each method performs 30 times on each problem independently, with IT_{max} is equal to 1000 and a search agent of 50. The control parameters of all algorithms are listed in Appendix B. In Table 1, the range of design variables for each model is listed. Each algorithm's efficiency is contrasted based on the RMSE values, convergence curve, and statistical data analysis.

4.1 Results of the PV cell and the PV module

This section discusses comprehensive experimental findings of the RTC France Si solar cell and PhotoWatt-PWP201 for both SDM and DDM. The lower the RMSE, the nearer the estimated value towards the experimental data, which indicates that the selected algorithm holds high efficiency in estimating unknown cell/module parameters. Thus, the error value tends to be reduced as low as possible. In the meantime, relative error (RE) and integral absolute error (IAE_i) are used to emphasize the value of the error between the experimental data and estimated data at each set value of the voltage, as described below.

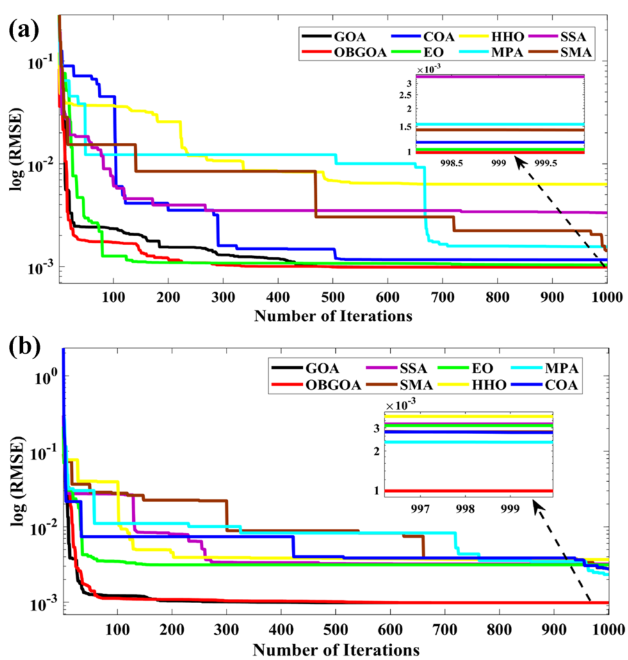

Fig. 5 Convergence curves of all algorithms (RTC France Si cell); **a** SDM, **b** DDM

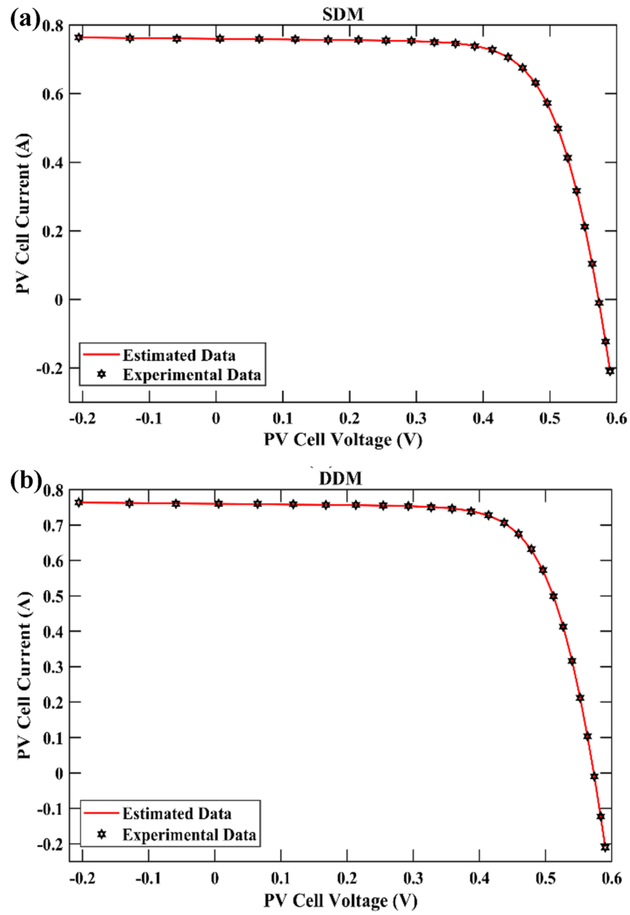

Fig. 6 I–V characteristics obtained by OBGOA (RTC France Si cell); **a** SDM, **b** DDM

$$RE = \frac{\left|I_{exp} - I_{est}\right|}{I_{exp}} \tag{35}$$

$$IAE_i = \left|I_{exp} - I_{est}\right| \tag{36}$$

where I_{exp} signifies the experimental current sample and I_{est} denotes the estimated current.

4.1.1 Results of the RTC France Si solar cell

By comparison, the reliability of the OBGOA has been dramatically increased relative to the standard GOA. Compared to several other techniques comprising COA, SSA, SMA, EO, HHO, MPA, GOA, as seen in Tables 2 and 3, the OBGOA obtained the best RSME with a result of 9.8602E – 04 for SDM and 9.8258E – 04 for DDM, suggesting that OBGOA is a robust tool for solving the problem of identification of uncertain parameters of the PV cell. The '+' sign in all tables indicates that the results obtained by

Table 4 Parameters estimated by various algorithms for SDM of the PV module (PhotoWatt-PWP201)

Algorithm	I_p (A)	I_{sd} (μA)	R_s (Ω)	R_p (Ω)	n	$RMSE$	sig
SSA	1.0303	3.8454E−06	1.1897	1048.174	49.02721	2.4440E−03	+
COA	1.0299	3.7314E−06	1.1945	1096.053	48.90762	2.4338E−03	+
SMA	1.0302	4.4740E−06	1.1723	1146.077	49.6259	5.5485E−03	+
EO	1.0286	4.1362E−06	1.1826	1343.376	49.30651	2.5106E−03	+
HHO	1.0315	5.2039E−07	1.3897	530.815	42.28063	7.3349E−03	+
MPA	1.0276	4.9237E−06	1.1672	1999.998	49.99995	2.5294E−03	+
GOA	1.0305	3.4823E−06	1.2013	981.982	48.64284	2.4251E−03	+
Proposed	**1.0305**	**3.4769E−06**	**1.2014**	**980.5942**	**48.6369**	**2.4115E−03**	

Table 5 Parameters estimated by various algorithms for DDM of the PV module (PhotoWatt-PWP201)

Algorithm	I_p (A)	I_{sd1} (μA)	R_s (Ω)	R_p (Ω)	n_1	I_{sd2} (μA)	n_2	$RSME$	sig
SSA	1.0297	6.2455E−10	1.1940	1126.068	1.064965	3.7641E−06	48.9408	2.6473E−03	+
COA	1.0290	6.7825E−10	1.1668	1490.589	47.62896	4.9127E−06	50.0000	4.2447E−03	+
SMA	1.0270	5.9259E−07	1.1886	1980.039	47.36756	3.7133E−06	49.9561	2.7059E−03	+
EO	1.0320	3.0165E−07	1.1743	889.969	47.93478	3.9363E−06	49.5645	2.4465E−03	+
HHO	1.0320	3.4382E−07	1.1779	898.776	47.458	3.7143E−06	49.2565	9.1295E−02	+
MPA	1.0313	4.9011E−06	1.1593	1052.676	50	2.41E−11	36.35096	2.6362E−03	+
GOA	1.0305	7.6813E−09	1.2016	983.195	47.90858	3.4675E−06	48.6367	2.4251E−03	+
Proposed	**1.0305**	**1.7557e−07**	**1.2010**	**982.0040**	**48.8085**	**3.3163e−06**	**48.6454**	**2.4018E−03**	

OBGOA are better than other algorithms. Figure 5 illustrates OBGOA's convergence curve and other selected algorithms, implying the value of mean RMSE after 30 individual runs of each algorithm for both SDM and DDM of the PV cell. Compared to other algorithms, OBGOA's convergence speed is excellent, i.e., early convergence to global minima. It is more straightforward to see that the convergence curve of the OBGOA has a better performance and is higher than other competitive algorithms. The OBGOA extracts the I–V characteristic of the SDM and DDM of the PV cell accurately, and it can be observed in Fig. 6. From Fig. 6, it is seen that the estimated data values and experimental data values are significantly suited over the experimental voltage points, which shows the reliability of the OBGOA and also, OBGOA's performance is significantly observed, and the current and power values are estimated from the experiment data. The RE and IAE between the experimental and simulated current at each voltage sample point are low enough to confirm that the OBGOA can reliably indicate solar cells' real characteristics. The value of IAE with respect to the current and power is calculated and listed in Tables 13 and 14 (refer Appendix A), respectively, for SDM and DDM, in addition to the value of RE at each experimental point. The boldface in all tables indicates the best values.

From Table 13, it is observed that the value of IAE is less than 1.627E−03, and the value of RE is less than 5.908E−03. The average values of IAE with respect to the power and current are 8.781E−05 and 7.225E−04, respectively, and the average value of RE is 4.507E−03, which indicates OBGOA can able to realize the real characteristics of the SDM. Table 14 displays explicitly that

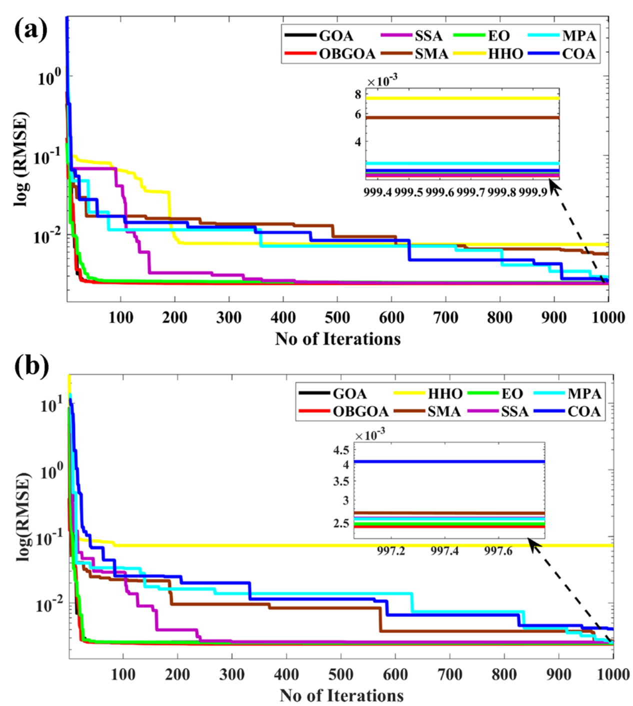

Fig. 7 Convergence curves of all algorithms (PhotoWatt-PWP201 PV module); **a** SDM, **b** DDM

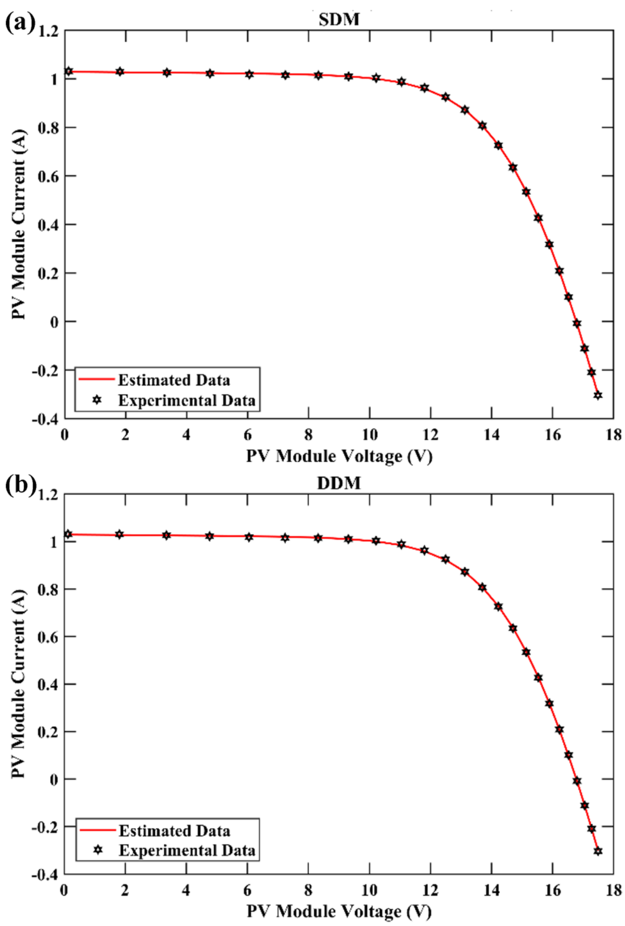

Fig. 8 I–V characteristics obtained by OBGOA (PhotoWatt-PWP201 module); **a** SDM, **b** DDM

the IAE (with respect to current and power) and RE values are smaller than 1.604E – 03 (with respect to current), 8.051E – 04 (with respect to current), and 6.957E – 03, respectively. The average values of IAE with respect to the power and current are 4.197E – 04 and 7.175E – 04, respectively, and the average value of RE is 7.536E – 05, which indicates OBGOA can able to realize the real characteristics of the DDM. Based on above-all discussions, it is claimed that OBGOA helps analyze both SDM and DDM model's unknown parameters.

4.1.2 Results of the PhotoWatt-PWP201 PV module

As in SDM/DDM of the PV cell, in SDM/DDM PV module model also the reliability of the OBGOA has been dramatically increased relative to the basic GOA version. Furthermore, compared to several other techniques, as seen in Tables 4 and 5, the proposed OBGOA obtained the best RSME with 2.4115E – 03 for SDM and 2.4018E – 03 for DDM, suggesting that OBGOA is a robust tool for solving the problem of identification of uncertain parameters of the PV model.

Figure 7 illustrates convergence curves, implying the value of mean RMSE after 30 individual runs of each algorithm for both SDM and DDM of the PhotoWatt-PWP201 PV module.

Compared to other techniques, OBGOA's convergence speed is excellent, i.e., early convergence to global minima. The proposed OBGOA extracts the I–V characteristic of the SDM and DDM of the PV module accurately, and it can be observed in Fig. 8. From Fig. 8, it is seen that the estimated data values and experimental data values are significantly suited over the experimental voltage points, which shows the reliability of the proposed OBGOA. The RE and IAE values are low enough to confirm that the OBGOA can reliably indicate the solar module's real characteristics. The value of IAE with respect to the current and power is calculated and listed in Tables 15 and 16 (refer Appendix A), respectively for SDM and DDM, in addition to the value of RE at each experimental point. From Table 15, it is observed that the value of IAE is less than 5.000E – 03, and the value of RE is less than 6.553E – 03. The average values of IAE with respect to the power and current are 5.599E – 03, and 0.0020, respectively, and the average value of RE is 1.0007E – 03, which indicates OBGOA can realize the real characteristics of the SDM. Table 16 displays explicitly that the IAE (with

Table 6 Average CPU time of various algorithms

Algorithm	RTC France Si cell		PhotoWatt-PWP201	
	SDM	DDM	SDM	DDM
SSA	2.6644E + 03	2.1536E + 03	2.2779E + 03	2.0654E + 03
COA	1.5842E + 03	1.3815E + 03	1.3110E + 03	1.3967E + 03
SMA	1.3895E + 03	1.3172E + 03	1.3165E + 03	1.3385E + 03
EO	2.5376E + 03	1.9629E + 03	1.8243E + 03	1.9226E + 03
HHO	1.6396E + 03	1.6234E + 03	1.3712E + 03	1.4196E + 03
MPA	2.2663E + 03	1.7908E + 03	1.7811E + 03	2.0042E + 03
GOA	**6.9845E + 02**	**6.0931E + 02**	**6.5623E + 02**	**6.3444E + 02**
Proposed	7.7547E + 02	6.3550E + 02	8.0140E + 02	6.6045E + 02

Table 7 Optimized variables by OBGOA for KC200GT PV module at a temperature of 25 °C

G (W/m^2)	I_p (A)	I_{sd} (A)	R_s (Ω)	R_p (Ω)	n	RMSE
1000	8.201	3.65E−09	0.337	498.03	1.101	0.0064
800	6.571	9.56E−10	0.357	743.84	1.035	0.0016
600	4.919	7.68E−09	0.323	465.13	1.141	0.0066
400	3.286	1.64E−09	0.349	805.96	1.060	0.0015
200	1.646	5.12E−10	0.382	687.33	1.002	0.0014

respect to current and power) and RE values are smaller than 4.415E−03 (with respect to current), 5.321E−02 (with respect to power), and 4.021E−02, respectively. The average values of IAE with respect to the power and current are 1.992E−02, and 0.0019, respectively, and the average value of RE is 5.534E−03, which indicates that OBGOA can realize the real characteristics of the DDM. Based on above-all discussions, it is claimed that OBGOA helps analyze both SDM and DDM model's unknown parameters. The above discussions show minimal IAE and RE between the estimated data and experimental data and are enough to show OBGOA reliability and solution accuracy.

4.1.3 Average run time

The computation cost is indeed a significant metric for assessing the efficiency of the algorithm. The average CPU computation time of all algorithms is reported in Table 6. From Fig. 9, it can be noticed that the time required by each method to address the problem on various models is different. The HHO has the highest total CPU time, no matter which model and the basic variant of GOA needs the shortest time. Even though OBGOA is not the fastest compared to GOA (better than other peers), other techniques are relatively similar to the OBGOA. Thus, it is declared that a more successful method is OBGOA.

4.2 Results of commercial PV modules

The authors wanted to investigate the feasibility of the OBGOA by defining SDM variables for two commercial PV modules, namely KC200GT and SM55. The KC200GT is a high-performance multi-crystalline module, and the SM55 is a monocrystalline module intended for industrial applications. The short-circuit current I_{sc} of the PV module finds the initial range of the I_p, the temperature coefficient of the short-circuit current is denoted as α, and the value is taken from the specification sheet. The value of I_{sc} is calculated using the datasheet at STC, and the expression to calculate I_{sc} is given as follows.

$$I_{sc}(T,G) = I_{sc-STC} \times \frac{G}{G_{STC}} + \alpha\left(T - T_{STC}\right) \tag{37}$$

where G and T denote the actual solar irradiance and temperature, G_{STC} and T_{STC} denote the solar irradiance and temperature at STC, and $I_{sc\text{-}STC}$ refers to the short-circuit current at STC.

The approximate findings of the five parameters for SDM of those two PV modules are listed in Tables 7, 8, 9 and 10. For such models, the OBGOA determines the optimal parameters at various irradiation levels (200 W/m^2, 400 W/m^2, 600 W/m^2, 800 W/m^2, and 1000 W/m^2) with a temperature of 25 °C. Similarly, the values of the parameters are

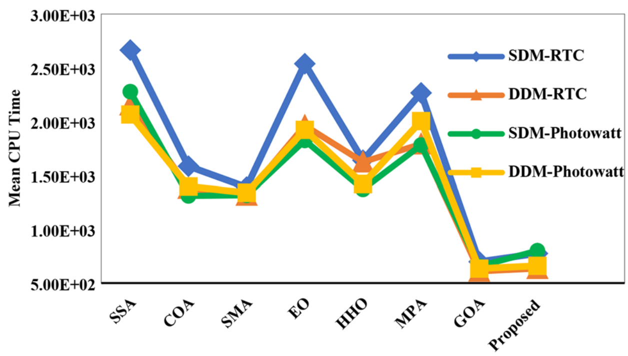

Fig. 9 Mean CPU time for different PV models

extracted for KC200GT at temperatures of 25 °C, 50 °C, and 75 °C, and SM55 at temperatures of 25 °C, 40 °C, and 60 °C with the solar irradiance of 1000 W/m^2. Figures 10, 11, 12 and 13 demonstrates the high degree of fitting under different operating conditions between the experimental value and estimated value of the two PV modules, presenting conclusive proof even further to demonstrate the effectiveness of the OBGOA.

4.2.1 Different solar irradiation conditions

Tables 7 and 8 lists the estimated parameters by OBGOA on different irradiation conditions for all two commercial PV modules. In Table 7, the estimated parameters for SDM of the KC200GT PV module by the proposed algorithm for different irradiation conditions. The I–V characteristics of KC200GT are shown in Fig. 10.

Table 8 shows the estimated parameters of the SM55 PV module by the OBGOA for different irradiation conditions. The I–V characteristics of SM55 are depicted in Fig. 11.

4.2.2 Different temperature conditions

Tables 9 and 10 lists the estimated parameters by OBGOA on different temperature conditions for all two commercial modules, similar to previous discussions. In Table 9, the estimated parameters of the KC200GT PV module by the proposed algorithm for different temperature conditions. The I–V characteristics of KC200GT for different temperatures are depicted in Fig. 12.

Table 10 shows the estimated parameters of the SM55 PV module by the proposed algorithm for different temperature conditions. The I–V characteristics of SM55 for different temperatures are depicted in Fig. 13.

The estimated value and experimental sample collected under different temperatures and different irradiation conditions fit well with all two PV modules. Therefore, the proposed OBGOA can achieve a low RMSE value on such test data sets. In addition, the I–V curves prove OBGOA's accuracy as the irradiance values, and temperature values differ. PV models encounter multiple environmental problems in actual situations, mainly as soon as the outdoor temperature is not appropriate or the solar irradiation is inadequate. Nevertheless, it can be seen in the findings that the OBGOA can

Table 8 Optimized variables by OBGOA for SM55 PV module at a temperature of 25 ℃

G (W/m^2)	I_p (A)	I_{sd} (A)	R_s (Ω)	R_p (Ω)	n	RMSE
1000	3.451	1.69E−07	0.329	482.36	1.395	0.0011
800	2.761	1.43E−07	0.337	459.85	1.381	6.68E−04
600	2.071	1.55E−07	0.330	450.86	1.387	8.23E−04
400	1.383	1.00E−07	0.396	427.46	1.352	7.05E−04
200	0.692	1.30E−07	0.312	438.08	1.371	5.20E−04

Table 9 Optimized parameters by OBGOA for KC200GT PV module at $G = 1000$ W/m^2

T (°C)	I_p (A)	I_{sd} (A)	R_s (Ω)	R_p (Ω)	n	RMSE
25	8.213	3.51E−09	0.336	992.47	1.099	0.0014
50	8.296	1.24E−07	0.336	908.03	1.117	0.0028
75	8.378	1.63E−06	0.343	790.35	1.106	0.0043

Table 10 Optimized parameters by OBGOA for SM55 PV module at $G = 1000$ W/m^2

T (°C)	I_p (A)	I_{sd} (A)	R_s (Ω)	R_p (Ω)	n	RMSE
25	3.447	3.63E−07	0.304	729.41	1.461	0.0012
40	3.469	1.22E−06	0.311	551.64	1.424	0.0036
60	3.495	6.92E−06	0.319	484.93	1.406	0.0037

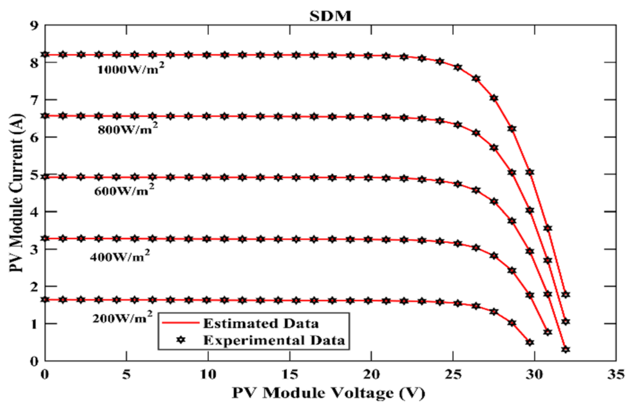

Fig. 10 I–V curves of KC200GT at various irradiations

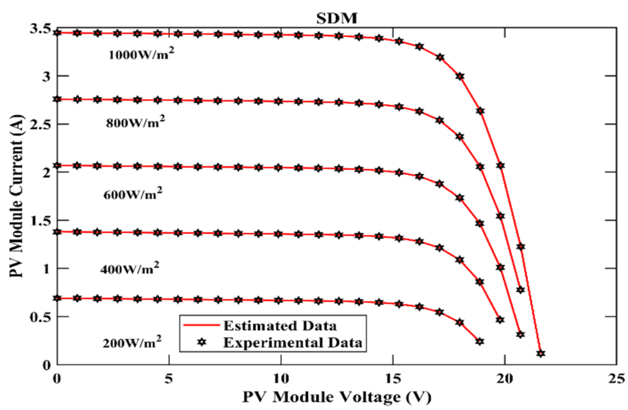

Fig. 11 I–V curves of SM55 at various irradiations

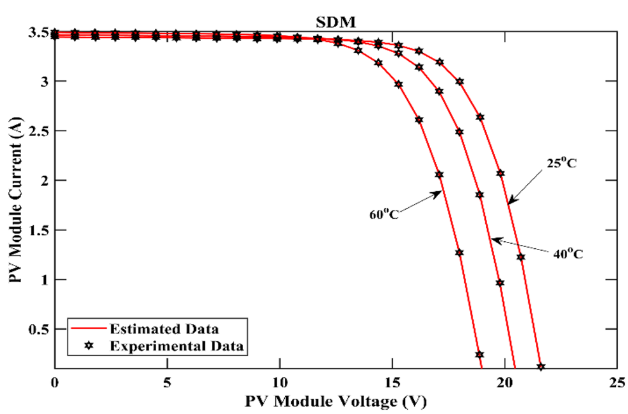

Fig. 13 I–V curves of SM55 at various temperatures

still achieve low RSME under low temperature and irradiance. In summary, it can reasonably be demonstrated that the OBGOA is an accurate and appropriate tool for obtaining unknown parameters under different irradiance and temperature conditions.

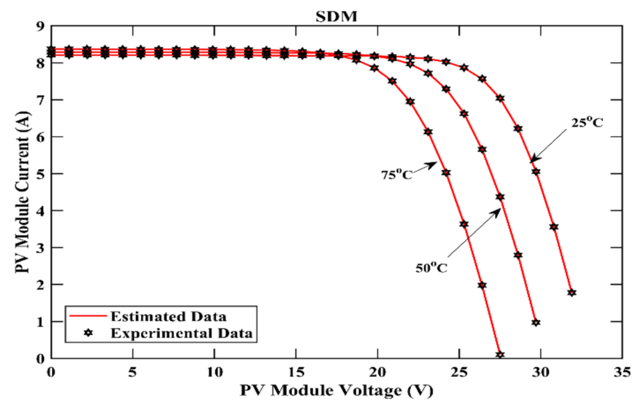

Fig. 12 I–V curves of KC200GT at various temperatures

4.3 Performance comparisons

Numerous comparisons and statistical measures with other existing techniques were performed to demonstrate the effectiveness of the OBGOA. Besides, the selection of these algorithms depends on choosing the most recent and efficient techniques that have been established to solve the problem of parameter identification in PV systems. The algorithms are SSA, COA, SMA, EO, HHO, MPA, and GOA, as discussed earlier. The statistical analysis has been carried out only for SDM/DDM of the PV cell, SDM/DDM of the PV module, and SDM of three commercial PV modules under different irradiation conditions as a sample analysis. The performance indicators, namely Min, Mean, Max, and SD values attained by different methods, are mentioned in Table 11 for the SDM and DDM. To rate the algorithms according to each evaluation metric, the rank (*R*) has been used. Considering the Min RMSE, it is evident that OBGOA finds the optimal RMSE with a value of 9.8602E − 4 for SDM and 9.8258E − 04 for DDM. Other methods have lower RMSE values, and with 8.796E − 3 for SDM and 3.7764E − 04, HHO is the worst method among various other methods. Besides, OBGOA reports a tremendous outperformance for the Mean and Max; in addition, the value of SD is also minimal compared to other algorithms. Few algorithms, such as HHO and SSA, display poor performance by examining the RMSE values. On the other hand, a few algorithms, such as MPA, SMA, COA, and EO, have demonstrated satisfactory results. The basic GOA also achieves the minimum RSME value, i.e., 9.929E − 04 for SDM and 9.8602E − 04 for DDM, but the OBGOA outperforms GOA in terms of Min, Mean, Max, and SD values and the remaining algorithms. Therefore, it is concluded that the OBGOA stands first for parameter estimation of the PV cell.

As similar to the statistical analysis of the RTC France Si cell, the PhotoWatt-PWP201 is also analyzed. The performance indicators attained by different methods are

Table 11 Statistical results of various algorithms for SDM/DDM of the RTC France Si cell

Model	Parameters	SSA	COA	SMA	EO	HHO	MPA	GOA	OBGOA
SDM	Min	2.093E – 03	1.102E – 03	1.382E – 03	1.051E – 03	8.796E – 03	1.522E – 03	9.929E – 04	**9.8602E – 04**
	Mean	3.487E – 03	5.748E – 03	3.732E – 03	2.374E – 03	2.545E – 03	6.454E – 03	2.045E – 03	**9.987E – 04**
	Max	1.489E – 02	1.675E – 02	9.851E – 03	4.786E – 03	8.388E – 02	8.577E – 03	1.155E – 03	**9.993E – 04**
	SD	3.874E – 03	4.55E – 03	3.993E – 03	3.514E – 03	1.045E – 03	8.57E – 04	5.577E – 04	**6.489E – 07**
	R	7	4	5	3	8	6	2	**1**
DDM	Min	3.1102E – 03	2.342E – 03	3.136E – 03	3.024E – 03	3.764E – 03	2.192E – 03	9.8602E – 04	**9.8258E – 04**
	Mean	3.824E – 03	6.65E – 03	4.48E – 02	4.56E – 03	2.245E – 02	3.13E – 03	4.24E – 03	**1.0254E – 03**
	Max	9.254E – 03	6.145E – 02	1.778E – 01	3.145E – 02	9.214E – 02	1.49E – 02	1.458E – 02	**1.214E – 03**
	SD	9.325E – 04	4.587E – 03	5.14E – 02	5.14E – 04	1.354E – 02	2.245E – 03	3.411E – 03	**5.689E – 05**
	R	6	4	7	5	8	3	2	**1**

Table 12 Statistical results of various selected algorithms for SDM/DDM of the PhotoWatt-PWP201

Model	Parameters	SSA	COA	SMA	EO	HHO	MPA	GOA	OBGOA
SDM	Min	2.444E – 03	2.433E – 03	5.548E – 03	2.511E – 03	7.335E – 03	2.529E – 03	2.425E – 03	**2.4115E – 03**
	Mean	4.697E – 03	3.987E – 03	2.625E – 03	**2.145E – 03**	3.858E – 02	3.458E – 03	2.887E – 03	2.425E – 03
	Max	2.98E – 01	2.457E – 02	3.147E – 02	4.871E – 02	2.741E – 01	3.114E – 02	3.921E – 03	**2.524E – 03**
	SD	1.478E – 04	1.025E – 04	3.47E – 04	2.325E – 03	9.877E – 03	1.998E – 04	1.145E – 04	**9.245E – 05**
	R	4	3	7	5	8	6	2	**1**
DDM	Min	2.647E – 03	4.244E – 03	2.706E – 03	2.446E – 03	9.339E – 02	2.636E – 03	2.425E – 03	**2.4018E – 03**
	Mean	3.745E – 03	6.285E – 03	4.984E – 03	1.143E – 02	3.114E – 02	3.698E – 03	2.701E – 03	**2.488E – 03**
	Max	9.692E – 03	1.447E – 02	8.557E – 03	2.476E – 02	3.694E – 01	1.452E – 02	3.742E – 03	**2.645E – 03**
	SD	2.14E – 04	1.65E – 04	2.474E – 04	3.21E – 03	8.87E – 03	1.74E – 04	1.698E – 04	**8.458E – 05**
	R	5	7	6	3	8	4	2	**1**

mentioned in Table 12 for the SDM and DDM. Considering the Min RMSE, it is obvious that OBGOA finds the optimal RMSE with a value of 2.4018E – 03 for SDM and 2.4115E – 03 for DDM. On the other hand, other methods have lower RMSE values, and with 7.335E – 03 for SDM and 9.339E – 02, HHO is the worst method among various other methods. Besides, OBGOA reports a tremendous outperformance for the Mean and Max; in addition, the value of SD is also minimal compared to other algorithms.

In Tables 11 and 12, a ranking of all the algorithms is provided. *R* provides the order of each method, considering the order of that algorithm relative to the other methods in all other parameters. As seen, OBGOA has the lowest R-value (1) and noticed that GOA performs second best, preceded by EO, SSA, COA, MPA, and SMA. As per the Min RMSE, in almost all situations, it is observed that the performance of OBGOA exceeds the other techniques, while OBGOA deservingly succeeds throughout all situations based on Mean RMSE.

The suggested algorithm is superior to all others in extracting the best parameters for the SDM, DDM, and PV module models with the help of the earlier observations and the statistical analysis of such outcomes, and the comparison with several other techniques. The proposed OBGOA can extract the variables of two commercial PV modules obtained from the supplier for practical application. It relies on many performance measures to estimate the effectiveness of OBGOA, including Min, Mean, Max, SD, computation time, and *R*. Especially compared to all algorithms except GOA, OBGOA is effective in terms of computation time. Besides, in terms of RMSE and *R*, OBGOA outperforms all existing algorithms. In addition to using an opposition-based learning scheme, the excellent results of OBGOA benefit from the strong exploration and exploitation abilities.

4.4 Discussions

This paper provides a robust approach for estimating the PV cell or PV module parameters to maximize its performance in solar photovoltaic systems. Considering the proposed method's findings, the proposed OBGOA estimates the value of the unknown variables promptly relative to the other techniques for the various PV models. The new algorithm significantly reduces the current and power losses relative to the experimental current and power. Furthermore, it is seen how the results indicate that the estimated values are very well adapted to the experimental values as the irradiance and the temperature levels are changed, and this is proof of the effectiveness of the proposed OBGOA. Besides, for real-time systems, OBGOA output is checked using commercial information retrieved from the datasheet provided by the manufacturers, such as the KC200GT and SM55. The proposed OBGOA is thus a conveniently applied and realistic solution, and it is an excellent alternative to identify the optimum parameters of the PV system. The average values of RMSE, SD, IAE, RE, and RT obtained by the proposed OBGOA have percentage decrease of 1.152%, 175%, 1.25%, 1.35%, and − 5%, respectively, with respect to the basic version of GOA. The average values of RMSE, SD, IAE, RE, and RT obtained by the proposed OBGOA have percentage decrease of 18%, 200%, 1.3%, 1.5%, and 50%, respectively, with respect to the other selected algorithms. It is worth stating that the proposed OBGOA finds exact parameters at various operating conditions, which is expressive for the maximum power point tracking of a photovoltaic system, since few modules in photovoltaic systems are subject to critical conditions, such as static shading, dynamic shading, and partial shading (Premkumar et al. 2021c; Manoharan et al. 2021). Besides, the obtained results can be utilized while modeling the maximum power point tracking system to track the maximum output power, as varying irradiation and temperature in real-time applications. The limitations of the proposed OBGOA are as follows. The computing efforts of OBGOA are greater than those for standard algorithms since more iterations are required, which might become computationally expensive if the simulation tool takes a long time to evaluate a single objective. Furthermore, the final solutions generated by OBGOA could be reproduced exactly; therefore, numerous runs must be performed to assure reliability and some relevant statistical analysis.

To summarize, the OBGOA has the highest SDM/DDM of PV cell and module convergence speeds. The enhanced capabilities in escaping local optima are because the OBL allows GOA to search optimal solutions faster than other widely used algorithms. As a result, the populations are less likely to become stuck in local optimal, achieving global optima more quickly than traditional approaches.

5 Conclusions

Identifying unknown parameters is a great challenge in photovoltaic systems to improve the accuracy of the power and current. This paper suggests an enhanced variant of the basic GOA to correctly predict the best parameters of the various models, such as SDM, DDM, and PV modules. In recent times, the OBL has gained further attention, which is used to enhance the effectiveness of heuristic methods. It has a significant characteristic that uses the basic variant of GOA to search in the solution space in the opposite direction to the current solution. The authors demonstrated the effect of OBL in this paper to enhance the accuracy of the GOA to solve the parameter estimation optimization problem. Numerous investigations were carried to allow contrasts with other state-of-the-art algorithms to evaluate the effectiveness of OBGOA. The findings and the statistical measures illustrate OBGOA's superior performance for all the various PV models in terms of RMSE, computation time, SD, RE, IAE, and R. Furthermore, the graphical illustration of the I–V curves shows that the estimated value is in good agreement with the experimental value. In addition, the effectiveness of OBGOA has been evaluated at various temperature and irradiance levels using data from the manufacturer's datasheet, and the OBGOA can be an alternative tool for parameter estimation of PV models.

The proposed method is expected to be extended in the future to many other energy sectors, such as PV array fault detection, PV array reconfiguration, maximum power point tracking, and energy scheduling in PV systems. Furthermore, the development of more successful strategies for the proposed method to be capable of solving several other optimization problems is also an ultimate goal, particularly for multi-objective and constrained problems. Additionally, the extension of the OBGOA to many other important topics, including image segmentation, feature selection problems, underwater targets classification, underwater acoustical dataset classification, multi-layer perceptron neural network trainer, and feed-forward neural network trainer, will be explored in the future.

Appendix A

See Tables 13, 14, 15 and 16. IAE_P denotes the integral absolute error with respect to the estimated power (P_{est}) and experimental power (P_{exp}) values.

Appendix B: control parameters of various algorithms

S. No.	Algorithm	Control parameters	Value
1	SSA	Number of search agents (N_p)	30 (SDM), 50 (DDM and others)
		Maximum number of iterations (IT_{max})	1000
		b	1
2	COA	Number of search agents (N_p)	10 packs with 30 coyotes for all problems
		Maximum number of iterations (IT_{max})	1000
3	SMA	Number of search agents (N_p)	30 (SDM), 50 (DDM and others)
		Maximum number of iterations (IT_{max})	1000
		V_b	− 1 to 1
4	EO	Number of search agents (N_p)	30 (SDM), 50 (DDM and others)
		Maximum number of iterations (IT_{max})	1000
		a_1, a_2, and RP	2, 1, and 0.5, respectively
5	HHO	Number of search agents (N_p)	30 (SDM), 50 (DDM and others)
		Maximum number of iterations (IT_{max})	1000
		β, F, and Q	1.5, 6, and 5, respectively
6	MPA	Number of search agents (N_p)	30 (SDM), 50 (DDM and others)
		Maximum number of iterations (IT_{max})	1000
		$FADs$, mutation probability, and p	0.5
7	GOA	Number of search agents (N_p)	30 (SDM), 50 (DDM and others)
		Maximum number of iterations (IT_{max})	1000
		P_r	0.5
8	OBGOA	Number of search agents (N_p)	30 (SDM), 50 (DDM and others)
		Maximum number of iterations (IT_{max})	1000
		P_r	0.5

Table 13 IAE and RE of OBGOA on SDM of the RTC France Si PV cell

Sample No.	Experimental values			Estimated current values			Estimated power values	
	V_{exp} (V)	I_{exp} (A)	P_{exp}(W)	I_{est} (A)	IAE_i (A)	RE_i (A)	P_{est} (W)	IAE_P (W)
1	− 0.2057	0.764	− 0.1571548	0.7641	1.118E − 04	1.463E − 04	− 0.157178	2.299E − 05
2	− 0.1291	0.762	− 0.0983742	0.7627	6.868E − 04	9.013E − 04	− 0.098463	8.866E − 05
3	− 0.0588	0.7605	− 0.0447174	0.7614	8.789E − 04	1.156E − 03	− 0.044769	5.168E − 05
4	0.0057	0.7605	0.0043349	0.7602	3.216E − 04	4.229E − 04	0.004333	1.833E − 06
5	0.0646	0.76	0.049096	0.7591	9.200E − 04	1.211E − 03	0.049037	5.943E − 05
6	0.1185	0.759	0.0899415	0.7580	9.329E − 04	1.229E − 03	0.089831	1.105E − 04
7	0.1678	0.757	0.1270246	0.7571	1.157E − 04	1.529E − 04	0.127044	1.942E − 05
8	0.2132	0.757	0.1613924	0.7561	8.338E − 04	1.101E − 03	0.161215	1.778E − 04
9	0.2545	0.7555	0.1922748	0.7551	3.885E − 04	5.142E − 04	0.192176	9.887E − 05
10	0.2924	0.754	0.2204696	0.7537	3.111E − 04	4.126E − 04	0.220379	9.098E − 05
11	0.3269	0.7505	0.2453385	0.7514	9.130E − 04	1.217E − 03	0.245637	2.985E − 04
12	0.3585	0.7465	0.2676203	0.7474	8.748E − 04	1.172E − 03	0.267934	3.136E − 04
13	0.3873	0.7385	0.2860211	0.7401	1.627E − 03	2.203E − 03	0.286651	6.300E − 04

Table 13 continued

Sample No.	Experimental values			Estimated current values			Estimated power values	
	V_{exp} (V)	I_{exp} (A)	P_{exp}(W)	I_{est} (A)	IAE_i (A)	RE_i (A)	P_{est} (W)	IAE_P (W)
14	0.4137	0.728	0.3011736	0.7274	5.666E−04	7.783E−04	0.300939	2.344E−04
15	0.4373	0.7065	0.3089525	0.7070	5.021E−04	7.107E−04	0.309172	2.196E−04
16	0.459	0.6755	0.3100545	0.6753	1.358E−04	2.010E−04	0.309992	6.232E−05
17	0.4784	0.632	0.3023488	0.6308	1.016E−03	1.607E−03	0.301863	4.860E−04
18	0.496	0.573	0.284208	0.5719	7.763E−04	1.355E−03	0.283823	3.850E−04
19	0.5119	0.499	0.2554381	0.4996	6.863E−04	1.375E−03	0.255789	3.513E−04
20	0.5265	0.413	0.2174445	0.4136	7.518E−04	1.820E−03	0.217840	3.958E−04
21	0.5398	0.3165	0.1708467	0.3175	1.049E−03	3.315E−03	0.171413	5.664E−04
22	0.5521	0.212	0.1170452	0.2122	5.109E−04	2.410E−03	0.117327	2.821E−04
23	0.5633	0.1035	0.0583016	0.1023	2.901E−04	2.803E−03	0.058138	1.634E−04
24	0.5736	−0.01	−0.005736	−0.0087	1.322E−03	1.322E−01	−0.004978	7.582E−04
25	0.5833	−0.123	−0.0717459	−0.1255	7.267E−04	5.908E−03	−0.072170	4.239E−04
26	0.59	−0.21	−0.1239	0.7641	1.535E−03	7.311E−03	−0.122994	9.058E−04
Sum of IAE	–	–	–	–	**7.225E−04**	**4.507E−03**	–	**8.781E−05**

Table 14 IAE and RE of OBGOA on DDM of the RTC France Si PV cell

Sample No.	Experimental values			Estimated current values			Estimated power values	
	V_{exp} (V)	I_{exp} (A)	P_{exp}(W)	I_{est} (A)	IAE_i (A)	RE_i (A)	P_{est} (W)	IAE_P (W)
1	−0.2057	0.764	−0.1572	0.7640	8.466E−05	1.108E−04	−0.1572	1.742E−05
2	−0.1291	0.762	−0.0984	0.7626	6.608E−04	8.672E−04	−0.0985	8.531E−05
3	−0.0588	0.7605	−0.0447	0.7613	8.539E−04	1.123E−03	−0.0448	5.021E−05
4	0.0057	0.7605	0.0043	0.7602	3.456E−04	4.544E−04	0.0043	1.970E−06
5	0.0646	0.76	0.0491	0.7591	9.431E−04	1.241E−03	0.0490	6.093E−05
6	0.1185	0.759	0.0899	0.7581	9.552E−04	1.259E−03	0.0898	1.132E−04
7	0.1678	0.757	0.1270	0.7572	9.393E−05	1.241E−04	0.1270	1.576E−05
8	0.2132	0.757	0.1614	0.7563	8.552E−04	1.130E−03	0.1612	1.823E−04
9	0.2545	0.7555	0.1923	0.7552	4.099E−04	5.426E−04	0.1922	1.043E−04
10	0.2924	0.754	0.2205	0.7537	3.330E−04	4.416E−04	0.2204	9.736E−05
11	0.3269	0.7505	0.2453	0.7514	8.906E−04	1.187E−03	0.2456	2.911E−04
12	0.3585	0.7465	0.2676	0.7473	8.519E−04	1.141E−03	0.2679	3.054E−04
13	0.3873	0.7385	0.2860	0.7400	1.604E−03	2.172E−03	0.2866	6.213E−04
14	0.4137	0.728	0.3012	0.7273	5.865E−04	8.057E−04	0.3009	2.426E−04
15	0.4373	0.7065	0.3090	0.7069	4.875E−04	6.900E−04	0.3092	2.132E−04
16	0.459	0.6755	0.3101	0.6752	1.424E−04	2.108E−04	0.3100	6.536E−05
17	0.4784	0.632	0.3023	0.6308	1.014E−03	1.604E−03	0.3019	4.849E−04
18	0.496	0.573	0.2842	0.5720	7.671E−04	1.339E−03	0.2838	3.805E−04
19	0.5119	0.499	0.2554	0.4997	6.974E−04	1.398E−03	0.2558	3.570E−04
20	0.5265	0.413	0.2174	0.4137	7.575E−04	1.834E−03	0.2178	3.988E−04
21	0.5398	0.3165	0.1708	0.3175	1.041E−03	3.290E−03	0.1714	5.621E−04
22	0.5521	0.212	0.1170	0.2121	4.811E−04	2.270E−03	0.1173	2.656E−04
23	0.5633	0.1035	0.0583	0.1022	3.482E−04	3.364E−03	0.0581	1.961E−04
24	0.5736	−0.01	−0.0057	−0.0088	1.230E−03	4.230E−03	−0.0050	7.058E−04
25	0.5833	−0.123	−0.0717	−0.1255	8.558E−04	6.957E−03	−0.0722	4.992E−04
26	0.59	−0.21	−0.1239	−0.2084	1.365E−03	6.498E−03	−0.1231	8.051E−04
Sum of IAE	–	–	–	–	**7.175E−04**	**4.197E−04**	–	**7.536E−05**

Table 15 IAE and RE of OBGOA on SDM of the PhotoWatt-PWP201 PV module

Sample No.	Experimental values			Estimated current values			Estimated power values	
	V_{exp} (V)	I_{exp} (A)	P_{exp}(W)	I_{est} (A)	IAE_i (A)	RE_i (A)	P_{est} (W)	IAE_P (W)
1	0.1248	1.0315	0.12873	1.0291	2.392E−03	2.319E−03	0.1284	2.985E−04
2	1.8093	1.03	1.86358	1.0274	2.630E−03	2.553E−03	1.8588	4.758E−03
3	3.3511	1.026	3.43823	1.0257	2.721E−04	2.653E−04	3.4373	9.120E−04
4	4.7622	1.022	4.86697	1.0241	2.090E−03	2.045E−03	4.8769	9.952E−03
5	6.0538	1.018	6.16277	1.0223	4.269E−03	4.194E−03	6.1886	2.585E−02
6	7.2364	1.0155	7.34856	1.0199	4.404E−03	4.337E−03	7.3804	3.187E−02
7	8.3189	1.014	8.43536	1.0164	2.339E−03	2.306E−03	8.4548	1.946E−02
8	9.3097	1.01	9.40280	1.0105	4.822E−04	4.775E−04	9.4073	4.490E−03
9	10.2163	1.0035	10.25206	1.0006	2.825E−03	2.815E−03	10.2232	2.886E−02
10	11.0449	0.988	10.91236	0.9845	3.340E−03	3.380E−03	10.8755	3.689E−02
11	11.8018	0.963	11.36513	0.9595	3.279E−03	3.405E−03	11.3264	3.870E−02
12	12.4929	0.9255	11.56218	0.9228	2.403E−03	2.596E−03	11.5322	3.002E−02
13	13.1231	0.8725	11.44990	0.8726	1.702E−04	1.950E−04	11.4521	2.233E−03
14	13.6983	0.8075	11.06138	0.8073	6.626E−05	8.205E−05	11.0605	9.076E−04
15	14.2221	0.7265	10.33236	0.7283	1.629E−03	2.242E−03	10.3295	2.844E−03
16	14.6995	0.6345	9.32683	0.6371	2.187E−03	3.447E−03	9.3224	4.410E−03
17	15.1346	0.5345	8.08944	0.5362	1.467E−03	2.745E−03	8.0879	1.513E−03
18	15.5311	0.4275	6.63955	0.4295	1.635E−03	3.826E−03	6.6349	4.659E−03
19	15.8929	0.3185	5.06189	0.3188	5.329E−04	1.673E−03	5.0603	1.589E−03
20	16.2229	0.2085	3.38247	0.2074	2.376E−04	1.140E−03	3.3786	3.855E−03
21	16.5241	0.101	1.66893	0.0962	2.203E−03	2.182E−02	1.6325	3.641E−02
22	16.7987	−0.008	−0.13439	−0.0083	5.242E−04	6.553E−03	−0.1377	3.360E−03
23	17.0499	−0.111	−1.89254	−0.1109	3.000E−03	3.750E−03	−1.9437	5.115E−02
24	17.2793	−0.209	−3.61137	−0.2092	5.000E−03	4.453E−04	−3.6978	8.640E−02
25	17.4885	−0.303	−5.29902	−0.3009	4.545E−04	2.389E−03	−5.3070	7.949E−03
Sum of IAE	–	–	–	–	**0.0020**	**5.599E−03**	–	**1.0007E−03**

Table 16 IAE and RE of OBGOA on DDM of the PhotoWatt-PWP201 PV module

Sample No.	Experimental values			Estimated current values			Estimated power values	
	V_{exp} (V)	I_{exp} (A)	P_{exp}(W)	I_{est} (A)	IAE_i (A)	RE_i (A)	P_{est} (W)	IAE_P (W)
1	0.1248	1.0315	0.1287312	1.0291	2.391E−03	2.318E−03	0.128433	2.984E−04
2	1.8093	1.03	1.863579	1.0274	2.627E−03	2.550E−03	1.858826	4.753E−03
3	3.3511	1.026	3.4382286	1.0258	2.670E−04	2.603E−04	3.437334	8.948E−04
4	4.7622	1.022	4.8669684	1.0241	2.097E−03	2.052E−03	4.876954	9.986E−03
5	6.0538	1.018	6.1627684	1.0223	4.279E−03	4.203E−03	6.18867	2.590E−02
6	7.2364	1.0155	7.3485642	1.0199	4.415E−03	4.348E−03	7.380516	3.195E−02
7	8.3189	1.014	8.4353646	1.0164	2.353E−03	2.321E−03	8.454939	1.957E−02
8	9.3097	1.01	9.402797	1.0105	5.000E−04	4.950E−04	9.407452	4.655E−03
9	10.2163	1.0035	10.252057	1.0006	2.803E−03	2.793E−03	10.22342	2.863E−02
10	11.0449	0.988	10.912361	0.9845	3.313E−03	3.354E−03	10.87577	3.660E−02
11	11.8018	0.963	11.365133	0.9595	3.248E−03	3.373E−03	11.3268	3.833E−02
12	12.4929	0.9255	11.562179	0.9228	2.368E−03	2.559E−03	11.53259	2.959E−02
13	13.1231	0.8725	11.449905	0.8726	2.061E−04	2.362E−04	11.45261	2.704E−03
14	13.6983	0.8075	11.061377	0.8073	3.119E−05	3.862E−05	11.06095	4.272E−04
15	14.2221	0.7265	10.332356	0.7283	1.661E−03	2.286E−03	10.35598	2.362E−02
16	14.6995	0.6345	9.3268328	0.6371	2.215E−03	3.491E−03	9.359393	3.256E−02

Table 16 continued

Sample No.	Experimental values			Estimated current values			Estimated power values	
	V_{exp} (V)	I_{exp} (A)	P_{exp}(W)	I_{est} (A)	IAE_i (A)	RE_i (A)	P_{est} (W)	IAE_P (W)
17	15.1346	0.5345	8.0894437	0.5362	1.491E−03	2.789E−03	8.112003	2.256E−02
18	15.5311	0.4275	6.6395453	0.4295	1.655E−03	3.871E−03	6.665246	2.570E−02
19	15.8929	0.3185	5.0618887	0.3188	5.493E−04	1.725E−03	5.070619	8.730E−03
20	16.2229	0.2085	3.3824747	0.2074	2.228E−04	1.069E−03	3.37886	3.614E−03
21	16.5241	0.101	1.6689341	0.0962	2.189E−03	2.167E−02	1.632765	3.617E−02
22	16.7987	−0.008	−0.1343896	−0.0083	3.217E−04	4.021E−02	−0.12899	5.404E−03
23	17.0499	−0.111	−1.8925389	−0.1109	1.000E−03	9.009E−03	−1.87549	1.705E−02
24	17.2793	−0.209	−3.6113737	−0.2093	3.079E−03	1.473E−02	−3.55816	5.321E−02
25	17.4885	−0.303	−5.2990155	−0.3009	2.000E−03	6.601E−03	−5.26404	3.498E−02
Sum of IAE	–	–	–	–	**0.0019**	**5.534E−03**	–	**1.992E−02**

Supplementary Information The online version contains supplementary material available at https://doi.org/10.1007/s12652-021-03564-4.

References

Abbassi R, Abbassi A, Heidari AA, Mirjalili S (2019) An efficient salp swarm-inspired algorithm for parameters identification of photovoltaic cell models. Energy Convers Manag 179:362–372

Abdel-basset M, Mohamed R, Mirjalili S et al (2020) Solar photovoltaic parameter estimation using an improved equilibrium optimizer. Sol Energy 209:694–708

Ahandani MA, Alavi-Rad H (2015) Opposition-based learning in shuffled frog leaping: an application for parameter identification. Inf Sci 291:19–42

Ahmadianfar I, Bozorg-haddad O, Chu X (2020) Gradient-based optimizer: a new metaheuristic optimization algorithm. Inf Sci 540:131–159

Allam D, Yousri DA, Eteiba MB (2016) Parameters extraction of the three diode model for the multi-crystalline solar cell/module using moth-flame optimization algorithm. Energy Convers Manag 123:535–548

Batzelis EI, Papathanassiou SA (2016) A method for the analytical extraction of the single-diode PV model parameters. IEEE Trans Sustain Energy 7:504–512

Biswas PP, Suganthan PN, Wu G, Amaratunga GAJ (2019) Parameter estimation of solar cells using datasheet information with the application of an adaptive differential evolution algorithm. Renew Energy 132:425–438

Chaibi Y, Malvoni M, Allouhi A, Mohamed S (2019) Data on the I-V characteristics related to the SM55 monocrystalline PV module at various solar irradiance and temperatures. Data Brief 26:104527

Chen H, Jiao S, Heidari AA et al (2019) An opposition-based sine cosine approach with local search for parameter estimation of photovoltaic models. Energy Convers Manag 195:927–942

Chin VJ, Salam Z, Ishaque K (2015) Cell modelling and model parameters estimation techniques for photovoltaic simulator application: a review. Appl Energy 154:500–519

Cuevas E, Oliva D, Zaldivar D, Pajares G (2012) Opposition-based electromagnetism-like for global optimization. Int J Innov Comput Inf Control 8:8181–8198

Diab AAZ, Sultan HM, Do TD et al (2020) Coyote optimization algorithm for parameters estimation of various models of solar cells and PV modules. IEEE Access 8:111102–111140

Drouiche I, Harrouni S, Hadj A (2018) A new approach for modelling the aging PV module upon experimental I – V curves by combining translation method and five-parameters model. Electr Power Syst Res 163:231–241

Hasanien HM (2015) Shuffled frog leaping algorithm for photovoltaic model identification. IEEE Trans Sustain Energy 6:509–515

Ishaque K, Salam Z (2011) An improved modeling method to determine the model parameters of photovoltaic (PV) modules using differential evolution (DE). Sol Energy 85:2349–2359

Ishaque K, Salam Z, Mekhilef S, Shamsudin A (2012) Parameter extraction of solar photovoltaic modules using penalty-based differential evolution. Appl Energy 99:297–308

Jamadi M, Merrikh-Bayat F, Bigdeli M (2016) Very accurate parameter estimation of single- and double-diode solar cell models using a modified artificial bee colony algorithm. Int J Energy Environ Eng 7:13–25

Jiao S, Chong G, Huang C et al (2020) Orthogonally adapted Harris hawks optimization for parameter estimation of photovoltaic models. Energy 203:117804

Jordehi AR (2016) Parameter estimation of solar photovoltaic (PV) cells: a review. Renew Sustain Energy Rev 61:354–371

Kaveh M, Khishe M, Mosavi MR (2019) Design and implementation of a neighborhood search biogeography-based optimization trainer for classifying sonar dataset using multi-layer perceptron neural network. Analog Integr Circuits Signal Process 100:405–428

Khanna V, Das BK, Bisht D et al (2015) A three diode model for industrial solar cells and estimation of solar cell parameters using PSO algorithm. Renew Energy 78:105–113

Khishe M, Mohammadi H (2019) Passive sonar target classification using multi-layer perceptron trained by salp swarm algorithm. Ocean Eng 181:98–108

Khishe M, Mosavi MR (2019) Improved whale trainer for sonar datasets classification using neural network. Appl Acoust 154:176–192

Khishe M, Mosavi MR (2020a) Classification of underwater acoustical dataset using neural network trained by chimp optimization algorithm. Appl Acoust 157:107005

Khishe M, Mosavi MR (2020b) Chimp optimization algorithm. Expert Syst Appl 149:113338

Khishe M, Safari A (2019) Classification of sonar targets using an MLP neural network trained by dragonfly algorithm. Wirel Pers Commun 108:2241–2260

Khishe M, Mosavi MR, Moridi A (2018) Chaotic fractal walk trainer for sonar data set classification using multi-layer perceptron neural network and its hardware implementation. Appl Acoust 137:121–139

Krishnakumar N, Venugopalan R, Rajasekar N (2013) Bacterial foraging algorithm based parameter estimation of solar PV model. In: 2013 Annual international conference on emerging research areas, AICERA 2013 and 2013 international conference on microelectronics, communications and renewable energy, ICMiCR 2013 – proceedings, pp 1–6

Kumar C, Raj TD, Premkumar M, Raj TD (2020) A new stochastic slime mould optimization algorithm for the estimation of solar photovoltaic cell parameters. Optik 223:165277

Kumari PA, Geethanjali P (2017) Adaptive genetic algorithm based multi-objective optimization for photovoltaic cell design parameter extraction. Energy Proc 117:432–441

Li S, Gu Q, Gong W, Ning B (2020) An enhanced adaptive differential evolution algorithm for parameter extraction of photovoltaic models. Energy Convers Manag 205:112443

Liang J, Ge S, Qu B et al (2020) Classified perturbation mutation based particle swarm optimization algorithm for parameters extraction of photovoltaic models. Energy Convers Manag 203:112138

Liao Z, Chen Z, Li S (2020) Parameters extraction of photovoltaic models using triple-phase teaching-learning-based optimization. IEEE Access 8:69937–69952

Long W, Cai S, Jiao J et al (2020) A new hybrid algorithm based on grey wolf optimizer and cuckoo search for parameter extraction of solar photovoltaic models. Energy Convers Manag 203:112243

Louzazni M, Khouya A, Amechnoue K, Craciunescu A (2017) Parameter estimation of photovoltaic module using bio-inspired firefly algorithm. In: Proceedings of 2016 international renewable and sustainable energy conference, IRSEC 2016, pp 591–596

Ma J (2014) Optimization approaches for parameter estimation and maximum power point tracking (MPPT) of photovoltaic systems, Thesis, University of Liverpool Repository, pp. 26–104. https://livrepository.liverpool.ac.uk/2006662/. Accessed 20 July 2020

Manoharan P, Subramaniam U, Babu TS et al (2021) Improved perturb and observation maximum power point tracking technique for solar photovoltaic power generation systems. IEEE Syst J 15:3024–3035

Mohamed N, Alrahim A, Yahaya NZ, Singh B (2013) Single-diode model and two-diode model of PV modules: a comparison. In: 2013 IEEE international conference on control system, computing and engineering, pp 210–214

Montoya OD, Gil-González W, Grisales-Noreña LF (2020) Sine-cosine algorithm for parameters' estimation in solar cells using datasheet information. J Phys Conf Ser 1671:012008. https://doi.org/10.1088/1742-6596/1671/1/012008

Mosavi MR, Khishe M (2017) Training a feed-forward neural network using particle swarm optimizer with autonomous groups for sonar target classification. J Circuits Syst Comput 26:1750185

Mosavi MR, Khishe M, Akbarisani M (2017) Neural network trained by biogeography-based optimizer with chaos for sonar data set classification. Wirel Pers Commun 95:4623–4642

Mosavi MR, Khishe M, Naseri MJ et al (2019) Multi-layer perceptron neural network utilizing adaptive best-mass gravitational search algorithm to classify sonar dataset. Arch Acoust 44:137–151

Navabi R, Abedi S, Hosseinian SH, Pal R (2015) On the fast convergence modeling and accurate calculation of PV output energy for operation and planning studies. Energy Convers Manag 89:497–506

Oliva D, Abd El Aziz M, Ella Hassanien A (2017) Parameter estimation of photovoltaic cells using an improved chaotic whale optimization algorithm. Appl Energy 200:141–154

Premkumar M, Babu TS, Umashankar S, Sowmya R (2020a) A new metaphor-less algorithms for the photovoltaic cell parameter estimation. Optik 208:164559

Premkumar M, Sowmya R, Mosaad MI, Abdul Fattah TA (2020b) Design and development of low-cost photovoltaic module characterization educational demonstration tool. Mater Today Proc. https://doi.org/10.1016/j.matpr.2020.09.135

Premkumar M, Sowmya R, Umashankar S, Jangir P (2020c) Extraction of uncertain parameters of single-diode photovoltaic module using hybrid particle swarm optimization and grey wolf optimization algorithm. Mater Today Proc. https://doi.org/10.1016/j.matpr.2020.08.784

Premkumar M, Sowmya R, Umashankar S, Pradeep J (2020d) An effective solar photovoltaic module parameter estimation technique for single-diode model. IOP Conf Ser Mater Sci Eng 937:012014

Premkumar M, Jangir P, Ramakrishnan C et al (2021a) Identification of solar photovoltaic model parameters using an improved gradient-based optimization algorithm with chaotic drifts. IEEE Access 9:62347–62379

Premkumar M, Jangir P, Sowmya R et al (2021b) Enhanced chaotic JAYA algorithm for parameter estimation of photovoltaic cell/modules. ISA Trans 116:139–166

Premkumar M, Kumar C, Sowmya R, Pradeep J (2021c) A novel salp swarm assisted hybrid maximum power point tracking algorithm for the solar photovoltaic power generation systems. Automatika 62:1–15

Qiao W, Khishe M, Ravakhah S (2021) Underwater targets classification using local wavelet acoustic pattern and multi-layer perceptron neural network optimized by modified whale optimization algorithm. Ocean Eng 219:108415

Rajasekar N, Krishna Kumar N, Venugopalan R (2013) Bacterial foraging algorithm based solar PV parameter estimation. Sol Energy 97:255–265

Sheng H, Li C, Wang H et al (2019) Parameters extraction of photovoltaic models using an improved moth-flame optimization. Energies 12:3527

Soliman MA, Hasanien HM (2020) Marine predators algorithm for parameters identification of triple-diode photovoltaic models. IEEE Access 8:155832

Tizhoosh HR (2005) Opposition-based learning: a new scheme for machine intelligence. In: Proceedings - international conference on computational intelligence for modelling, control and automation, CIMCA 2005 and international conference on intelligent agents, web technologies and internet, vol 1, pp 695–701

Venkata Rao R (2016) Jaya: a simple and new optimization algorithm for solving constrained and unconstrained optimization problems. Int J Ind Eng Comput 7:19–34

Verma OP, Aggarwal D, Patodi T (2016) Opposition and dimensional based modified firefly algorithm. Expert Syst Appl 44:168–176

Wolf P, Benda V (2013) Identification of PV solar cells and modules parameters by combining statistical and analytical methods. Sol Energy 93:151–157

Wolpert DH, Macready WG (1997) No free lunch theorems for optimization. IEEE Trans Evol Comput 1:67–82

Wong WK, Ming CI (2019) A review on metaheuristic algorithms: recent trends, benchmarking and applications. In: 2019 7th International conference on smart computing and communications, ICSCC 2019, pp 1–5

Xiong G, Zhang J, Shi D, He Y (2018a) Parameter extraction of solar photovoltaic models using an improved whale optimization algorithm. Energy Convers Manag 174:388–405

Xiong G, Zhang J, Yuan X et al (2018b) Parameter extraction of solar photovoltaic models by means of a hybrid differential evolution with whale optimization algorithm. Sol Energy 176:742–761

Yang X-S, Deb S (2010) Cuckoo search via levy flights. In: World congress on nature & biologically inspired computing (NaBIC), IEEE, Coimbatore, India, pp 210–214

Yu K, Chen X, Wang X, Wang Z (2017a) Parameters identification of photovoltaic models using self-adaptive teaching-learning-based optimization. Energy Convers Manag 145:233–246

Yu K, Liang JJ, Qu BY et al (2017b) Parameters identification of photovoltaic models using an improved JAYA optimization algorithm. Energy Convers Manag 150:742–753